Review

Remote Sensing Techniques in Monitoring Post-Fire Effects and Patterns of Forest Recovery in Boreal Forest Regions: A Review

Thuan Chu * and Xulin Guo

Department of Geography and Planning, University of Saskatchewan, Saskatoon, SK S7N5C8, Canada; E-Mail: xulin.guo@usask.ca

* Author to whom correspondence should be addressed; E-Mail: thuan.chu@usask.ca; Tel.: +1-306-966-1488; Fax: +1-306-966-5680.

Abstract: The frequency and severity of forest fires, coupled with changes in spatial and temporal precipitation and temperature patterns, are likely to severely affect the characteristics of forest and permafrost patterns in boreal eco-regions. Forest fires, however, are also an ecological factor in how forest ecosystems form and function, as they affect the rate and characteristics of tree recruitment. A better understanding of fire regimes and forest recovery patterns in different environmental and climatic conditions will improve the management of sustainable forests by facilitating the process of forest resilience. Remote sensing has been identified as an effective tool for preventing and monitoring forest fires, as well as being a potential tool for understanding how forest ecosystems respond to them. However, a number of challenges remain before remote sensing practitioners will be able to better understand the effects of forest fires and how vegetation responds afterward. This article attempts to provide a comprehensive review of current research with respect to remotely sensed data and methods used to model post-fire effects and forest recovery patterns in boreal forest regions. The review reveals that remote sensing-based monitoring of post-fire effects and forest recovery patterns in boreal forest regions is not only limited by the gaps in both field data and remotely sensed data, but also the complexity of far-northern fire regimes, climatic conditions and environmental conditions. We expect that the integration of different remotely sensed data coupled with field campaigns can provide an important data source to support the monitoring of post-fire effects and forest recovery patterns. Additionally, the variation and stratification of pre- and post-fire vegetation and environmental conditions should be considered to achieve a reasonable, operational model for monitoring post-fire effects and forest patterns in boreal regions.

1. Introduction

Forests are subject to a variety of disturbances that are themselves strongly influenced by climate change and human activities [1]. Forest disturbance by fires is a major challenge for forest management in various ecosystems, due to the loss of lives and infrastructure, greenhouse gas emissions, soil degradation, soil erosion and the destruction of species, biomass and biodiversity [1–4]. On the other hand, forest fires constitute one major ecological process, especially during the initial stages of forest regeneration, which positively influences rapid growth in young trees, early and abundant seed germination and the dispersal of seeds [5]. Wildfire is also the most important factor controlling forest age structure, species composition, forming landscape pattern and influencing energy flows and biogeochemical cycles [6]. Forest fires and fire regimes, however, are severely underreported at a global and regional scale. Only 78 countries responding to fire effect surveys, representing 63 percent of the global forest area, reported that 60 million hectares of land, including forests and other wooded land, were burned per year throughout 2003–2007 [1]. According to the Food and Agriculture Organization [1], additional information is needed on the dynamics of fire in ecological forests, their direct and underlying causes and impacts and the desired long-term condition of ecosystems, such as forest structure and the composition and health of species.

The boreal forest is the largest forest biome and accounts for one third of global forest cover [7] across Scandinavia, Russia, Alaska and northern Canada. Boreal regions store more carbon in trees, soil and peat than any other terrestrial ecosystem [6], so they contribute largely to forest products consumed by human populations and play a significant role in controlling global climate. These forests have been influenced and shaped by natural disturbances, such as fires, extreme weather and insect infestations [8–11]; of these, wildland fire is the most widespread, and yet, it is an important, natural part of maintaining boreal forest ecosystems [7,12]. However, the ecological effects of boreal forest fires are highly variable, difficult to predict and are influenced by fire regimes, vegetation cover, permafrost condition, topography, soil properties and local climate [7,13–15]. An example of this is the potential shift in dominant evergreen conifer forests to deciduous forests in North America due to high fire severity and frequency in the last two decades [16]. Such disturbance-driven changes have potential feedbacks that may exacerbate or mitigate regional and global climate change [12,16,17], as well as influence carbon cycle [18] and forest biodiversity [19]. Monitoring both the impact of boreal fires and how boreal forests respond to changing environmental conditions is therefore a key element of forecasting and mitigating the negative effects of global change.

Remote sensing techniques for forest fire prevention, assessment and monitoring have been developing since the mid-1980s [20]. These techniques have been employed to address three different temporal fire-effects phases: pre-fire conditions, active fire characteristics and post-fire ecosystem responses [20–23]. Numerous algorithms and approaches for the first two phases have been developed [24–33]; little effort, however, has yet been dedicated to assessing suitable remote sensing

data and methods over the widely spatial and temporal ranges of post-fire-affected environments, particularly in characterizing and evaluating the patterns of how forest ecosystems respond to fire disturbances [2,20,34].

This paper reviews the methods and remotely sensed data used for modeling post-fire effects and forest recovery patterns, with a greater focus on examples of boreal forests, as well as the existing optical remote sensing data and methods that can be potentially applied to the aftermath of fires in this ecosystem. This paper will first examine the terminology and the ecological impacts of fire in controlling the recovery of post-fire boreal forest ecosystems, then will look at the recent remote sensing methods and data that have been applied in the literature for mapping the post-fire effects of burned areas and burn severity in boreal forest regions. It will also focus on remote sensing methods and data for modeling post-fire recovery patterns, including forest successional stages, forest structural attributes and the trajectory of forest regrowth following fire disturbance in boreal eco-regions. In each review section, this paper assesses the advantages and benefits of applying the remote sensing approach in monitoring post-fire boreal forests. Last, it examines existing remote sensing studies on post-fire effects and forest recovery patterns, which allows for the anticipation of some sources of uncertainties and limitations of such research, then suggests opportunities and future directions of monitoring post-fire boreal forests through the use of remote sensing.

2. Forest Fire/Forest Pattern Terminology and Review Method

2.1. Forest Fire and Forest Pattern Terminology

Climate condition, forest fuels, ignition agents, topography and human activities are five major factors that strongly influence forest fire activity and forest dynamics [35–38]. Forest fires, in turn, impact climate conditions, plant ecosystems and human life [2,3,39], and vegetation responds and adapts to changes in the environment by establishing an appropriate structure and composition as a consequence [40–43]. As with any endeavor involving different disciplines, an understanding of the terminology used throughout the study of the process and phenomenon of post-fire effects and forest patterns is essential within this review.

Within the fire science community, there are a variety of terms used to describe the characteristics of fire and its effects. The current review is associated with some of these terms: pre-fire environment, fire environment, active fire, post-fire environment, fire regimes defined by fire intensity, fire and burn severity, season of burn, type of fire and burned size and shape. Here, the review follows Jain *et al.* [44] , Key and Benson [45], Lentile *et al.* [20], French *et al.* [21] and Veraverbeke *et al.* [46], who accepted these terms as follows (Table 1, [9,20,21,44,47–83]). A schematic representation of the fire-related environment's relationship and assessment of post-fire effects on a forest's condition is shown in Figure 1.

Table 1. Definitions of fire-related environments and parameters used to measure fire/post-fire effects and forest patterns. When assessing post-fire environments, there are some fire characteristics, such as fire frequency and fire season, which are necessary to take into account in order to understand post-fire effects and forest patterns.

Fire-Related Environment	Parameter	Definition of Parameter	Selected Study/Reference
Pre-environment	-	The environmental characteristics of a site before the fire.	[21,44,47–50]
Fire environment: The environmental characteristics of a site during a fire. This is the state involved with active fire.	Fire frequency/fire recurrence	Number of fires per unit of time in a specified area. This is the temporal aspect of fire regimes.	[51–55]
	Fire intensity	A description of fire behavior quantified by energy release, such as temperature and heat from burning organic matter.	[16,20,56–58]
Post-environment: The environmental characteristics of a site after a fire, including both short- and long-term effects.	Burned area and fire perimeter	The measurement of post-fire effects in terms of dimension/area; affected area by fire or spatial extent of fire effect.	[20,59–65]
	Fire severity	The degree of environmental change caused directly by fire assessing immediately after a fire event (an initial assessment). This is the short-term severity assessment.	[16,20,58,66–69]
	Burn severity	The degree of environmental change caused by fire, assessed by a certain amount of time elapsed after a fire (an extended assessment). This includes both short- (e.g., pre-recovery phase after fire) and long-term post-fire severity (e.g., the observed changes in the characteristics of vegetation regrowth after fire, such as re-sprouting or regeneration); frequently used by remote sensing applications.	[20,21,46,69–77]
	Forest structure	Post-fire arrangement and distribution of forest components (e.g., seedling density, tree height, tree diameter, Leaf Area Index)	[74,78,79]
	Forest composition	Post-fire characteristics of species richness and abundance	[78,80]
	Forest function	Post-fire production of organic matter by the recovery forest.	[78,81]
	Forest succession	Different stages of vegetation recovery following fires.	[9,82,83]

As an agent of change to accelerate the modification of vegetation landscape, forest fires control both environments for vegetation establishment and vegetation succession [82,84,85]. In coupling regional climates with ecotope conditions, fire characteristics determine post-fire forest structure, composition and function [82,86,87] (Table 1). The spatial arrangement and distribution of forest components, such as the height of different canopies and tree diameter, define forest structure. Forest composition, however, is characterized by species richness and abundance as a description of forest biodiversity. Finally, forest function refers to the production of organic matter [78]. According to Franklin *et al*. [88] and Pommerening [79], the above structural, compositional and functional attributes of a forest are interdependent. For example, species composition and abundance can be surrogates of structural and functional attributes, such as canopy layering, decomposition and nutrient

cycling processes. This review uses a general term of *forest pattern* to represent the response of a forest ecosystem to disturbance by fire and climate change in which the forest pattern is formed by the forest structure and forest composition and is measured by the distribution, arrangement and number of different species or forest types after the disturbances. Furthermore, throughout this review, vegetation recovery, regrowth, regeneration and succession are occasionally used interchangeably. They all refer to the recovery process of a forest stand from a non-stand replacement fire disturbance or the reestablishment of a new forest stand from a stand-clearing fire disturbance. More specifically, forest succession is mainly observed in a broader context of forest ecosystem responses and that refers to the different stages of vegetation recovery post-disturbances in this review. Examples of some possible stages of forest recovery following fire disturbance are bare land, grass dominance species, forest tree germination and seedling and young, mature and old forest stands.

> **Figure 1.** Schematic representation of fire-related environments and assessment of post-fire effects on forest conditions concerning this comprehensive review. This review will particularly focus on studies of post-fire environments with respect to remote sensing approaches.
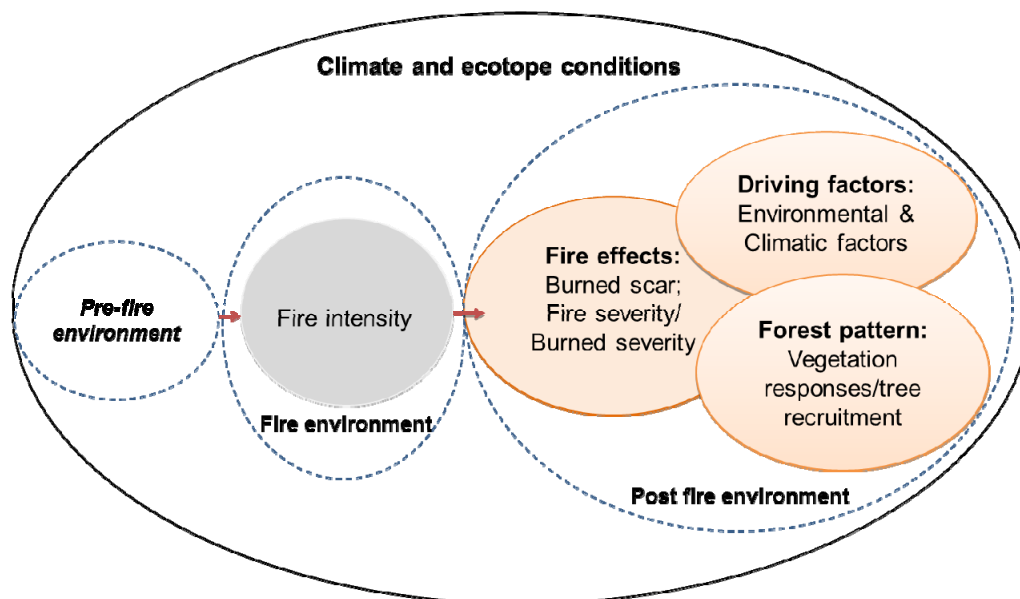
Depending on the forest composition and structure, species ecology and climate and ecotope condition, boreal forest fire regimes influence post-fire recovery patterns (Figures 1 and 2). An example of this is how North American boreal conifer forests have gradually shifted to broadleaf deciduous forests as a result of high fire severity [16]. Regarding fire frequency, Sofronov and Volokitina [19] assumed that an absence of fires during a very long period may lead to a gradual degradation of forest vegetation, due to the increase in the moss and duff layer, which would subsequently exacerbate poor soil conditions. Rare fire frequency approximately once in a century can act as a natural factor on boreal forests that allows the existence of stable forest vegetation and relatively high biodiversity of plants in boreal forest ecosystems; high and very high fire frequency, occurring once in 20–30 yr and 3–5 yr, respectively, are likely to act as a destructive factor [19]. High fire frequency may lead to the replacement of the forest vegetation by nonarboreal vegetation, such as

meadow, shrub or tundra, or even take fifty to hundreds years to recover to pre-fire conditions [9,89]. Post-fire soil properties, soil organic layer depth and permafrost-related soil moisture are also major factors that help determine the patterns of boreal forest recovery. Kasischke *et al*. [90] found that post-fire black spruce seedling density positively correlated with the organic layer depth remaining after the fire, while the depth of organic layers negatively affected aspen recruitment and growth. These patterns of tree recruitment in post-fire boreal forests are further affected by soil moisture [90], soil burn severity and pre-fire spruce and aspen basal area and drainage [74]. The review based on those boreal fire characteristics, ecological factors and post-fire tree recruitment patterns (Figure 2) discusses some challenges and research opportunities using remote sensing data and methods for monitoring post-fire boreal forests. This review will therefore focus only on the previous studies of post-fire environments with respect to applications for remote sensing on mapping post-fire effects and forest recovery patterns.

Figure 2. A brief schematic diagram of the relationships between ecological factors, fire effects and their influence on the recovery of post-fire boreal forests in permafrost ecosystems. Post-fire forest recovery patterns can be defined by factors directly available to the plant, such as light (e.g., solar radiation), water (e.g., soil moisture) and mechanical factors (e.g., fire regime). The review will focus on the interrelationship between those drivers in order to discuss the challenges and research opportunities in monitoring post-fire boreal forests using remote sensing.
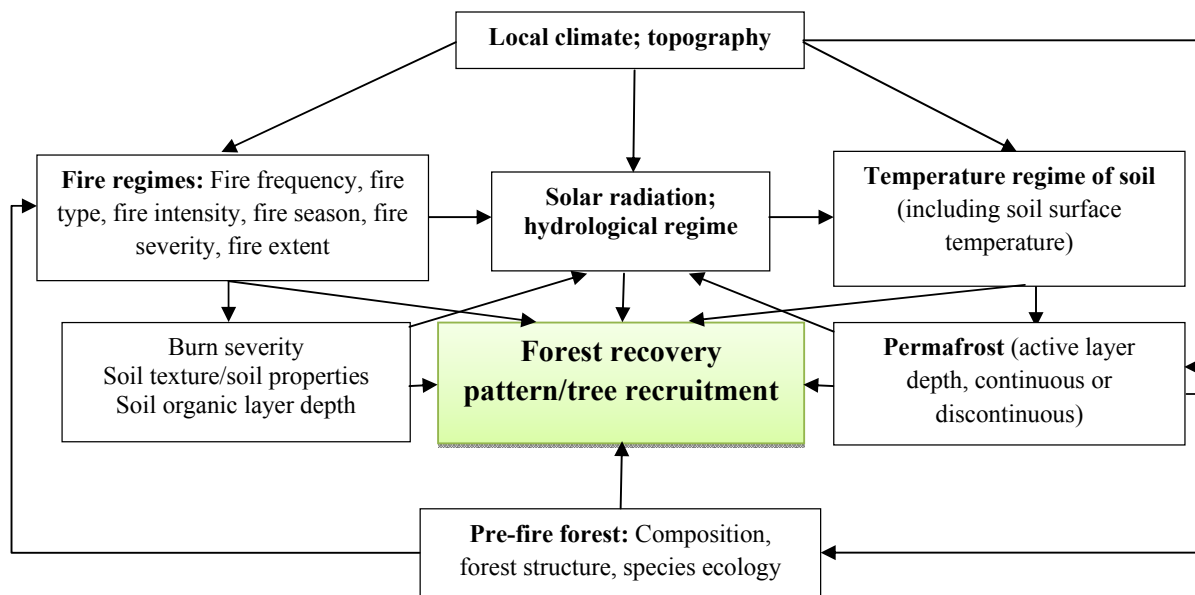
2.2. Review Methodology

Some keywords were defined, such as burned area mapping, burn severity, post-fire, boreal forest, remote sensing and forest recovery, based on review objectives, fire- and forest-related environment terminology, remote sensing techniques and boreal forest regions. Consequently, more than 200 articles published from 1989 to 2013 were chosen after thorough searches in several electronic databases, including ScienceDirect, Scopus, SpringerLink, Google[TM] Scholar and Web of Science. Almost all of the articles that were searched were published in journals related to remote sensing

(116 articles), as well as forest ecology and wildland fires (90 articles). Very few papers from conference proceedings have been taken into account. Each article was examined and catalogued by burned area and burn severity mapping, forest succession monitoring, forest structural attributes monitoring and trajectory of post-fire forest recovery. In each topic, we also grouped papers that examined similar remote sensing methods and data, as well as studies in different boreal zones, such as Alaska, Canada and Siberia, in order to discuss the strengths and limitations of studies related to post-fire boreal forests using remote sensing. Even though several of these studies were not conducted in post-fire boreal zones, they are included in this review, because their remote sensing techniques can be potentially applied to post-fire boreal forest research. Along with general conclusions and recommendations in the last section of this review, specific advantages, limitations, research gaps and solutions for both post-fire effects in boreal forests and the monitoring of forest patterns using remote sensing can be found at the end of each reviewed section.

3. Monitoring Post-Fire Effects and Forest Recovery Patterns Using Remote Sensing

3.1. Burned Area Mapping

3.1.1. Remote Sensing Data and Derived Products for Burned Area Mapping

In studies of post-fire effects, burned area mapping is one of the most common uses of remote sensing and is very well documented at a local, regional and global level. It provides timely, cost-effective and spatially comprehensive views of both areas that have been affected by fire and their pattern of occurrence [20,91]. At local scales in boreal regions, high to moderate resolution sensors, such as Landsat Thematic Mapper and Enhance Thematic Mapper Plus (Landsat TM/ETM+) [92–94] and radar imagery [95,96] have been employed for mapping burned areas. On the other hand, medium to coarse satellite data have been commonly used for regional and global analyses of burned areas, including boreal regions (Tables 2 and 3, [61,63–65,93–123]). The National Oceanic and Atmospheric Administration (NOAA) Advanced Very High Resolution Radiometer (AVHRR) images, for example, were mainly used as data for assessing the effects of fires during the 1990s and early 2000s [61,65,100,108,110,113–115,117,118,120,124]. The Moderate Resolution Imaging Spectrometer (MODIS) [64,98,99,121,122,125–130] and the Systeme Pour I'Observation de la Terre Vegetation (SPOT VEGETATION) [101,110,112,116,131–133] have been widely used more recently for both detecting active fires and mapping burned scars due to their high quality of temporal and spectral resolution and the availability of data since 2000 and 1998, respectively. In addition to the processing of raw satellite data for burned areas, several products derived from burned areas at a global scale are available to users, including the Moderate Resolution Imaging Spectroradiometer global burned area (MODIS MCD)45A1 and MCD64A1 products [102,123,126,127], Global Fire Emissions Database (GFED) [103,134], the global vegetation burned area product 2000–2007 (L3JRC) [104,131], the Global Land Products for Carbon Model Assimilation (GLOBCARBON) [105,135], the **G**lobal Monitoring for Environment and Security integrating **E**arth **O**bservation related to **Land** Cover and Vegetation (GEOLAND)-2 [106,136] and the Global Burnt Surface (GBS) product [104,137] (Table 2).

Table 2. Examples of optical remote sensing data for reconstructing and monitoring burned areas in boreal forest regions. All the derived products of burned areas are covered globally and can be downloaded from the web resources. The raw satellite data, such as Systeme Pour I'Observation de la Terre (SPOT), Landsat, Moderate Resolution Imaging Spectroradiometer (MODIS) and Advanced Very High Resolution Radiometer (AVHRR), require preprocessing and applying burn algorithms to derive burned areas. TM, Thematic Mapper; ETM+, Enhance Thematic Mapper Plus; ASTER, Advanced Spaceborne Thermal Emission and Reflection Radiometer; LAC, Local Area Coverage; LTDR, Long-Term Data Record; PAL, Pathfinder Land; GFED, Global Fire Emissions Database; NOAA, National Oceanic and Atmospheric Administration.

Satellite/ Derived Product	Sensor	Temporal Coverage	Temporal Resolution	Spatial Resolution	Spectral Bands (µm)	Web Resources
SPOT	HRV	1986–present	26 days	2.5–20 m	VIS–MIR (0.55–1.66)	-
Landsat	MSS, TM, ETM+, 8	1972–present	16 days	15–120 m	VIS–MIR (0.44–2.2; TIR (10.9,12)	[94]
Terra	ASTER	2000–present	16 days	15–90 m	VIS–MIR (0.56–2.34); TIR (8.3,−11.3)	[97]
Terra and Aqua	MODIS	2000–present	Daily	250 m, 500 m. 1 km	VIS–MIR (19 bands); TIR (17 bands)	[98,99]
NOAA	AVHRR (LAC/HRPT, GAC, LTDR, PAL)	1978–present	Daily	1.1 km, 4 km, 5 km, 8 km	VIS–MIR (0.63–3.74); TIR (11,12)	[100]
SPOT	SPOT VEGETATION	1998–present	Daily	1.15 km	VIS–MIR (0.55–1.62)	[101]
MODIS active fire	MODIS (MOD14, MYD14)	2000–present	5 min, daily, 8 day	1 km	-	[98,99]
MODIS burned area product	MODIS (MCD45A1, MCD64A1)	2000–present	Monthly	500 m	-	[102]
GFED	MODIS 500, TRIM/VIRS, ATSR	1995 to present	Daily, monthly, annual	0.25° (GFED4); 0.5° (GFED3)	-	[103]
L3JRC	SPOT VEGETATION	2000–2007	Daily	1 km	-	[104]
GLOBCARBON	SPOT VEGETATION, ATSR-2, AATSR	1998–2007	Monthly	1 km	-	[105]
GEOLAND-2	SPOT VEGETATION	1999–present	10 days	1 km	-	[106]
GBS	NOAA-AVHRR GAC	1982–1999	Weekly	8 km	-	[104]

Currently, the Advanced Very High Resolution Radiometer (AVHRR) represents the only remote sensing dataset capable of reconstructing long-term burned areas (since 1978) for almost all forest regions [121]. Unfortunately AVHRR data, with their low spatial and spectral resolution, vary greatly in terms of radiometric stability, cloud cover, transmission problems and distortion among different regions and timelines [121]. Although Landsat TM/ETM+ data, which offers greater spectral, spatial and radiometric resolution than AVHRR, have been widely used for mapping burned areas [92,93,138], these data are not always available in most countries at a regional scale, in addition to the gap of data in 2011 and 2012. Thus, the MODIS [98,99] and ASTER [97] data, available from 2000 onward, with its higher spatial and spectral resolution and quality of data possibly make it suitable to combine with

AVHRR and Landsat data for reconstructing long-term burn trends at different spatial scales. This also requires examining a suitable method of remote sensing for gathering data in reconstructing long-term burned areas.

Table 3. Summary of studies on mapping burned areas in local and regional boreal regions using the remote sensing approach. dNBR, Differenced Normalized Burn Ratio; NDVI, Normalized Difference Vegetation Index; SAR, spaceborne synthetic aperture radar; ERS, European Remote Sensing;VGT, Vegetation; RMSE, Root Mean Square Error.

Study	Boreal Zone	Period of Burned Area	Remote Sensing Data and Method	Validation Method	Results
Kasischke *et al.* [107]	Alaska	1990	AVHRR-NDVI composite from single-season	Compared with data from the Alaska Fire Service	Detected 89.5% of all fires greater than 2,000 ha; mapped only 61% of fires mapped by the field observers
Cahoon *et al.* [108]	Northern China and southeastern Siberia	1987	AVHRR-GAC and unsupervised minimum distance classification	Compared with Landsat TM image	Good agreement between the most intensively burned areas
French *et al.* [109], Kasischke and French [65]	Alaska	1990 and 1991	AVHRR-NDVI composite from two-season	Compared with data from the Alaska Fire Service	Detected more than 80% of fire greater than 2,000 ha; detected > 78% of the burned areas mapped by the field observers
Bourgeau-Chavez *et al.* [96]	Alaska	1979–1992	ERS-1 SAR backscatter (1991–1994) and ground burn relationship	Compared with data from the Alaska Fire Service	Detected 58% of the total burn area; detected up to 91% of the burn area using combined method of ERS-1 and AVHRR
Fraser et al. [110]	Canada	1995–1996	AVHRR-HRPT Hotspot and NDVI Differencing Synergy (HANDS algorithm)	Compared with official fire statistics	Detected > 95% of the total burn area; provided a consistent means of mapping large burns (>10 km^2)
Remmel and Perera [111]	Ontario, Canada	1992,1993, 1995	AVHRR-NDVI change detection methods by [65,107]	Assessed by the ground-truthed information	Detected > 65% of all fires in 1992 and 1993, but only 30% of fires detected in 1995
Bourgeau-Chavez *et al.* [95]	Sites in Canada and central Russia	1989–1996	C-band SAR backscatter, similar method in [96]	Validated with fire service records	RMSE = 7%–35% for the Canadian study sites; not validated for the Russian sites
Fraser and Li [112]	Canadian boreal forest	1998–1999	Normalize Shortwave-based Vegetation Index (SWVI) from SPOT VEGETATION	Validated with official burn records	Detected about 85% of the burned areas compiled by the Canadian Fire Centre
Li *et al.* [113]	Canada	1994–1998	AVHRR-HRPT hotspots analysis	Compared with official fire statistics	Underestimated 35% of the total burned area

Table 3. *Cont.*

Study	Boreal Zone	Period of Burned Area	Remote Sensing Data and Method	Validation Method	Results
Kajii *et al.* [114]	Siberia and northern Mongolia	1998	AVHRR-HRPT 12 hotspots	-	Large fires (>100 km^2) accounted for 90% of the total burned area
Kelha *et al.* [115]	Eurasia boreal region	1999–2000	AVHRR-HRPT and ATSR hotspots analysis	Evaluated by official fire records	False alarm rate from 7% to 12%
Soja *et al.* [117]	Siberia	1996–2000	AVHRR-HRPT hotspots analysis	Compared with Russian fires statistics	Underestimated by an average of 213%
Sukhinin *et al.* [118]	Russia and Easter Russia	1995–1997 and 1995–2002	AVHRR-HRPT active-fire analysis; defined burned area by aggregating fire pixels into polygons	Validated by official burned-area statistics	Overestimated two to five times compared with the burned-area statistics
George *et al.* [63]	Central Siberia	1992–2003	Combined MODIS SWIR and thermal anomaly data (STANDD)	Compared with Landsat ETM+ dataset	Overall accuracy of 81% with a kappa coefficient of 0.63
Loboda *et al.* [119]	Northern Eurasia	2001–2004	MODIS active fire and cluster identification to define burned areas	Compared with Landsat ETM+ dataset and other studies	Consistent results with the Landsat burned area and the other studies
Loboda *et al.* [64]	Central Siberia	2001–2002	dNBR threshold from MODIS MOD09A1 images	Compared with Landsat ETM+ dataset	Kappa values from 0.35 to 0.79, depending on fire scar magnitude
Pu *et al.* [120]	North America	1989–2000	AVHRR hotspots analysis applied to HANDS algorithm [110]	Compared with official statistics	Depending on the year; 40%–75% for omission and 18%–32% for commission error
Chuvieco *et al.* [121]	Western Canada	1984–2006	Ten-day composites of AVHRR-LAC and two-phase approach	Compared with official statistics and other studies	10% and 50% of commission and omission error, respectively
Potapov *et al.* [93]	North America and Eurasia	2000–2005	Combination of MODIS and Landsat data to analyze forest cover loss	Validated using the independently-derived Landsat burned area	RMSE of 2.24% and R^2 of 0.75
Loboda *et al.* [122]	Alaska	2004–2007	Pre-season and post-season dNBR threshold from MODIS MOD09A1	Compared with monitoring trends in burn severity products	Overall accuracy of 90%–93% and kappa of 0.67–0.75
Vivchar [123]	Russia	2000–2008	Analysis of MODIS MCD45 burned area product	Compared with other published results	Varied depending on the observed year
Moreno Ruiz *et al.* [61]	Canada	1984–1999	AVHRR-LTDR and Bayesian network classifier	Compared with other products and fire perimeters	Correlated well with fire event records, R^2 = 0.65

Because the accuracy of long-time series data of burned areas is important for modeling fire emissions and assessing feedback between fires and global climate change [139], the use of products derived from global burned areas, such as MODIS burned area products, GFED, L3JRC, GLOBCARBON and GEOLAND-2, at local and regional scales requires validation prior to applying the products at local and regional scales. Comparisons and critical reviews of the accuracy of those different burned areas' products are well reported in the literature [62,129,140]. Giglio *et al.* [129] found that there were considerable differences in many regions among burned area products of the GFED, the L3JRC global data from burned areas, the GLOBCARBON burned area product and the Collection 5 MODIS

MCD45A1 burned area product. The burned area reported in the L3JRC product was much higher than all other datasets in almost all regions, except for Africa, while the GFED product was most closely similar to the MCD45A1 dataset. Kasischke *et al*. [62] also found that the GFED version 3 (GFED3) burned area product was the most consistent source of burned area when compared to the fire management data in North America, whereas L3JRC and GLOBCARBON products significantly overestimated burned areas. The MCD45A1 dataset underestimated and resulted in a higher fraction of burned area compared to the GFED3 data [62]. Similarly, Kukavskaya *et al*. [139] found that estimates of burned areas in the region of Siberia from 2000 to 2011 differed significantly and were inconsistent within the data sources. MODIS MCD64A1 reported the smallest area burned for almost the whole year from 2000 to 2011, whereas the estimates from the combination of AVHRR and MODIS burned area product (AVHRR/MODIS) [117,118] were consistently greater than the MCD45A1 and MCD64A1 products by 6%–560% [139]. The great variation among burned area estimates in the region of Siberia have been accounted for through the instrument capabilities (e.g., resolution, cloud cover, fire types detection), differing methods of analysis and the absence of official data for the calibration and validation of burned areas [139]. These suggest that the use of global burned area products for local and regional scales should be validated and compared with other independent datasets (e.g., higher resolution datasets and official fire data) to quantify omission/commission errors. This also indicates a strong need to improve computer and Earth observation facilities to achieve a higher quality of burned area products using remote sensing for remote boreal regions.

3.1.2. Remote Sensing Methods, Results and Limitations for Burned Area Mapping

Changes in spectral signatures that occur following a fire can be surrogates for identifying patterns of burned areas. When vegetation is burned, there is a drastic reduction in visible-to-near-infrared reflectance and an accompanied increase in the short and middle infrared surface reflectance of most satellite sensors [20,141]. Burned patches are relatively easy to discriminate visually [142] for this reason. They are complex to detect automatically, however, because of the wide range of spectral signatures and spatial heterogeneity caused by fire regimes, the type of vegetation burned and the environmental conditions [59,122,142,143]. Table 3 summarizes studies on mapping burned areas in boreal forests to indicate some gaps in the research of burned areas in this region, as almost all studies used medium to coarse resolution data of AVHRR, MODIS and SPOT VEGETATION sensors to derive burned areas. Due to the absence of official data on burned areas, some studies in Eurasian boreal regions validated the derived burned area products using the higher resolution dataset of the Landsat satellite [63,64,116,119], while the results of the North American studies were compared with the official fire records [61,107,109,111,120,121].

The accuracy of estimates for burned areas vary significantly among those studies, even in the same study area and period, and are confounded by differing methods of analysis and sources of data (Table 3). For example, Chuvieco *et al*. [121] generated a 23-yr period of burned areas in western Canada using 10-day composites of AVHRR data and found that the results of mapping burned areas showed a significant underestimation compared with official statistics, due to a high omission error of 50%. Chuvieco *et al*. [121] reported a lower variation of omission and commission errors in the four sampled years (1989, 1994, 1995 and 1998), ranging from 47% to 65% for omission and 6% to 19%

for commission compared with 40% to 75% omission and 18% to 32% commission in Pu *et al.*'s [120] results for the same years. The proportion of total burned area in western Canada identified by the Chuvieco *et al.* study showed more consistency with the official records than that reported by the Pu *et al.* results, ranging from 50% to 68% and from 38% to 96%, respectively. Additionally, Moreno Ruiz *et al.* [61] compared the existing AVHRR burned area products in Canada and found that both AVHRR LTDR (Long-Term Data Record) and AVHRR LAC (Local Area Coverage) data substantially underestimated the total burned area in western Canada, both annually and throughout the year. The LTDR algorithm by Moreno Ruiz *et al.* [61] predicted 65% of total burned areas between 1984 and 1999, compared to the LAC product by Chuvieco *et al.* [121] of 53% in the same sampled years. Both the LTDR and LAC products showed a high consistency with the Canadian Forest Service National Fire Database (CFSNFD) pattern in western Canada, while the global AVHRR-PAL (Pathfinder Land) burned area product [144] did not track the CFSNFD pattern.

A number of techniques have been developed to map burned surfaces, ranging from visual interpretation with single channel or synthetic bands [145] to semi-automatic and automatic burned area classification algorithms [59,110,121,122,146]. In general, Chuvieco *et al.* [121] grouped algorithms for discriminating between burned areas into two categories: single processing chains and two-phase processing chains. The former commonly uses image classification techniques to discriminate burned and unburned areas, such as supervised and unsupervised classification, decision trees and differencing and thresholding of spectral indices [64,65,107–109,113,122]. However, in the two-phase approach, core burned areas are first defined from the most severe burn pixels based on active fire pixels or the threshold of vegetation indices, and then, contextual algorithms are employed to refine the classification of burn scars [121,125,142,147,148]. As shown in Table 3, the use of satellite data, such as AVHRR and MODIS, to detect hotspots during the period of interest has been widely applied to monitor burn areas in many studies in the boreal regions, since the hotspots represent burn activity. The detection of hotspots can be seen as the first step in defining the most severe burn pixels in the two-phase approach that was first introduced by Fraser *et al.* [110] (Hotspot and NDVI Differencing Synergy (HANDS) algorithm) to map burned areas in boreal regions. In the HANDS algorithm by Fraser et al. [110], hotspots were detected using thresholds on the brightness temperature of AVHRR channel 3 [113] and the AVHRR NDVI difference of pre-fire and post-fire composites. The confirmed hotspots were then used to derive coarse, regional and local-level NDVI difference thresholds for mapping burned areas [110]. The inclusion of both hotspot and NDVI differencing strategies aimed to use the strengths of each method to compensate for their limitations when mapping burned areas. However, the authors noted that the use of NDVI differencing to confirm hotspots, as well as to develop burn thresholds in the HANDS algorithm may result in a high commission error caused by a decrease in NDVI unrelated to fire [110,121]. The decrease of NDVI in some areas might be due to background noise, such as snow cover and vegetation senescence [110]. In addition to NDVI, Chuvieco *et al.* [121] used Global Environmental Monitoring Index (GEMI), Burned Area Index (BAI) and near-infrared reflectance of 10-day composite AVHRR data to confirm hotspot pixels, as well as to analyze the context of the surrounding seed pixels for mapping a time series of burn areas in Canada using the two-phase approach. The results of the study by Chuvieco *et al.*'s showed a very low commission error of 10%, but a high omission error of 50%. According to Chuvieco *et al.* [121], this high omission tendency may be accounted for through the geometric and

radiometric quality of the AVHRR dataset, making it very difficult to apply a consistent algorithm to the whole time series.

According to Bastarrika *et al*. [142], the two-phase approach can improve burn scar discrimination by solving contradictions between omission and commission errors in mapping burned areas, compared with the one-phase approach (Table 4). This approach, however, may not yield a consistent pattern when applying a long-time series of an AVHRR dataset for reconstructing burned areas, as shown in the study by Chuvieco *et al*. [121]. More studies are therefore needed in different regions using other satellite datasets to confirm the strengths of the two-phase approach. A quantitative comparison between the performance of the areas of the world with limited satellite and remote sensing applications are also needed (Table 4).

Several studies in boreal forest regions noted that the mapping of burned areas in such high northern latitudes using remote sensing should account for the variations of fire season, vegetation phenomenon, timing of burned area measurement and climatic and environmental conditions in order to attain a high quality dataset of the burn area [59,61,64,92,122,149]. All information related to vegetation, fire and environment can be obtained from remote sensing data (e.g., fire regimes from MODIS products [7], vegetation phenology from AVHRR-NDVI analysis [150]) and can be subsequently incorporated into mapping algorithms to improve the accuracy of mapping burned areas (Table 4). Loboda *et al*. [64] developed a regionally adaptable MODIS dNBR (Different Normalized Burn Ratio)-based algorithm for mapping burned areas in the boreal forests of central Siberia with the consideration of regional specifics of fire occurrence and vegetation properties. The dNBR was calculated using the NBR values in the compositing period containing the fire scar and the same two compositing periods one year prior and then following the fire year in order to account for the phenology-driven intra-annual variability of the vegetation state [122]. Thresholds of dNBR for burned area mapping in central Siberia were also derived depending upon the percentage of tree cover in which dNBR thresholds were set at 300 (dNBR × 1,000) for areas with tree cover > 10% and 200 for areas with tree cover ≤ 10% [64]. Recent changes in Alaska in fire regimes showed that the amount of area burned during late-season fires increased over the past two decades and accounted for 35% of total burned areas in the 2000s [149]. These late-season fires also burned deeper surface organic layers in Alaska's boreal forest that significantly affect a forest's post-fire recovery [14,90,149]. For this reason, mapping burned areas caused by late-season fires is important in ecological studies of forest ecosystems, such as Alaska's boreal forest. However, mapping late-season fires in such high northern latitudes is challenging, because of the limitations in data and environmental conditions [122]. A possible solution proposed by Loboda *et al*. [122] is an ecosystem-based burned mapping approach using pre-fire, fire and post-fire season spring composites to account for late-season fires and to fill in the gap left by the lack of sufficient clear land surface observations in high northern latitudes, due to cloud cover and cloud shadow, high aerosols in the atmosphere and the presence of snow on the ground. Similar to the employment of multi-temporal composite images by Loboda *et al*. [122], Moreno Ruiz *et al*. [61] calculated the differences of the AVHRR Burned Boreal Forest Index (BBFI) and AVHRR-GEMI from the year of the fire and the years before and after to detect burned areas in the Canadian boreal forest based on empirical thresholds and the Bayesian network classifier. The authors suggested that the application of the Bayesian network classifier for mapping burned areas should consider the recovery rate of forests, as well as the inclusion of high-to-moderate satellite imagery (e.g., Landsat) to ensure reliable training sites for the

algorithm. A similar methodology by Loboda *et al.* [122] and Moreno Ruiz *et al.* [61] can be applied to other boreal regions with the consideration of fire season and forest recovery rate to maximize the performance of burn algorithms. The overall strengths and limitations of remote sensing data and methods for mapping burned areas in boreal regions are given in Table 4.

Table 4. Strengths and limitations of some remote sensing data and methods for mapping burned areas in boreal regions.

Data/Method	Strength	Limitation and Notice for Use	Reference
High-to-moderate spatial resolution data (e.g., Landsat, ASTER, SPOT)	-High accuracy compared with fire management data; -A number of developed algorithms; -Good independent dataset for validating burned area products from lower resolution data; -Local scale	-Gap of data in some regions and some periods (e.g., Russian boreal forest); -Requires combination with lower spatial resolution data (e.g., MODIS and AVHRR) for reconstructing long-time burn series; -Necessary to find suitable algorithms for data integration	[92,93]
Moderate-to-coarse spatial resolution data and global burned area products (e.g., AVHRR, MODIS)	-Long-time series with high temporal resolution; -Available to use derived products (e.g., MOD45A1, GFED, L3JRC, GLOBCARBON); -Regional-to-global scales	-Considerable differences among burned area products; -High variation of omission/commission errors depending on the methods of analysis and regions; -Required calibration and validation with other independent datasets (e.g., higher resolution data) to apply to local and regional scales; -Required regional algorithms for mapping burned areas in high northern latitudes of boreal forest due to the limitations of data and environmental conditions. as well as complex fire regimes (e.g., fire season)	[61,62,93,122,129,140]
Single processing approach	-A number of available algorithms to apply, such as supervised/unsupervised classification, object-based classification, decision tree and regression tree models; differencing and thresholding of vegetation indices; -Simple and time saving for data processing	-Diverse omission and commission errors in different methods and ecosystems; -Result depends on the selection of the training dataset; -Proposed algorithms may be inapplicable to other study sites; -Required composite images of pre-fire year, fire year and post-fire year to account for variations of fire regimes and vegetation phenology	
Two-phase processing approach	-Solved contradictions between omission and commission errors associated with over- and under-estimation; -An alternative to automate mapping burned areas at a country scale	-Required strong detection of seed burned pixels for the first phase to ensure the lowest commission error; -The second phase depends on the spatial configuration of the seed pixels; -Uncertainty about low commission and omission errors using long-time series of datasets with low resolution data (e.g., AVHRR); -Need more studies in boreal ecosystems with different satellite datasets; -Need to compare with other methods	

3.2. Burn Severity Assessment

Burn severity is a function of physical and ecological changes caused by both short- and long-term post-fire effects [20,151]. It thus can be used to measure the levels of response from a post-fire forest ecosystem, as it is often assumed that areas with a high burn severity are positively correlated with the increasing mortality of vegetation and water repellency and, then, negatively correlated with the vegetation's ability to rehabilitate [21,22,152]. The impact on ecosystem functions of burn severity, however, also depends on the pre-fire environment and vegetation types [20]. Therefore, the mapping of burn severity provides information that gives insight into the cover patterns of post-fire vegetation [153] and also helps to guide forest managers in conducting their restoration efforts [154].

3.2.1. Field-Based Measurement of Burn Severity

Lentile *et al*. [20] summarized that field-based measures of post-fire effects include an assessment of changes in soil color, soil infiltration and hydrophobicity and changes in vegetation cover, which can be consistent and quantifiable indicators in remotely sensed data. Key and Benson [45], for example, introduced the ground-based Composite Burn Index (CBI) to integrate a variety of those different post-fire effect indicators for assessing burn severity. This index was developed as an operational methodology for assessing burn severity on a national scale in the U.S., in the framework of the FIREMON (Fire Effects Monitoring and Inventory Protocol) project [73]. The CBI is based on a visual assessment of the quantity of fuel consumed, the degree of soil charring and the degree of tree mortality and is assigned into one numeric site index assessed over a plot (e.g., about 30–60 m in diameter) [76]. The severity based on CBI has often been fire effect variations estimated in low, moderate and high classes across regions and vegetation types, such as in temperate regions [155–158] and boreal regions [66,76]. In Alaskan boreal forests, Kasischke *et al*. [66] found that the CBI was an important variable for estimating mineral soil exposure, while there were low correlations between CBI and other measures of fire severity, including the post-fire depth of organic layers. These results indicate that the CBI approach may not be appropriate for measuring fire/burn severity in the Alaskan boreal forest ecosystem, since the consumption of the organic layer by fire is an important factor in evaluating the response from vegetation and tree recruitment after fire disturbance in this ecosystem [14,66,74]. More studies on the performance of CBI in other boreal regions of the world are needed to compare with the CBI-based assessment of burn severity in the Alaskan boreal region.

Additionally, the CBI is also inconsistent with remotely sensed data in some ecosystems due either to spectral reflectance variation among different ecosystems or the performance of spectral indices used to determine CBI [67,158,159]. De Santis and Chuvieco [158] developed the Geo Composite Burn Index (GeoCBI) to improve the retrieval of burn severity from remotely sensed data. The modified version of the CBI takes into account the fraction of coverage (FCOV) of the different vegetation strata and changes in the Leaf Area Index (LAI) of the intermediate and tall tree data. For different ranges of burn severities, GeoCBI is more strongly correlative to spectral reflectance than CBI [158]. Recently, the Weighted Composite Burn Index (WCBI) [138,155] and the Post Fire Index (PFI) [160] have also been proposed to estimate burn severity and post-fire soil conditions from field measurements, as well as to validate remote sensing measurements. Burn severity can also be assessed

by visual interpretations and categorizing the characteristics of post-fire vegetation and soil, including the proportion of live trees, tree mortality, basal area [151,161,162], fuel biomass reduction and canopy mortality [163], Leaf Area Index [164] and the number of standing tree death and trees down, soil exposure and organic layer depth [66,74,77].

3.2.2. Remote Sensing Indices as Independent Variables to Estimate Burn Severity

Recent studies have demonstrated the sensitivity of spectral bands and indices of remotely sensed data to changes in burn severity classes (Table 5 and Figure 3), similar to mapping burned areas. Spectral indices, such as the Normalized Burn Ratio (NBR) and NDVI have been widely used for assessing burn severity through remote sensing in boreal regions [67,69,76,165,166]. Analyses of burn severity and burned area using multi-temporal satellite data and bi-temporal image differencing techniques have also resulted in the numerous differenced indices for burn severity assessment in boreal regions, such as the Differenced Normalized Burn Ratio (dNBR) [69–71,76,83,165,167–169], the Differenced Normalized Difference Vegetation Index (dNDVI) [76,170] and a relative version of the dNBR (RdNBR) [138]. The above listed indices are often independent variables used to derive dependent field-based indices of burn severity, such as CBI and WCBI [71,76,138,165,168,171], and post-fire organic soil layer depth [67,166], to estimate burn severity at the pixel level. The correlation between remote sensing indices and field-based measurements of burn severity depends upon various factors, such as the timing of the assessment of fire and burn severity, local environment conditions and characteristics of the vegetation. For example, Epting *et al.* [76] evaluated 13 remotely sensed indices, including single bands, band ratios, vegetation indices and multivariate components across four wildfire burn sites in Alaska and found that the NBR was the best for estimating burn severity. However, the NBR was useful as an index of burn severity for only forested sites in Alaska, since the correlation between NBR and CBI was low in non-forested classes. Similar results were also investigated by other studies in boreal forests that indicated a significant correlation between NBR/dNBR and CBI with respect to the surface plant community [71,77,166], the severity of canopy-layer fire rather than the severity of ground-layer [69], pre-fire conditions [83] and topographic conditions [75]. These results suggest that the assessment of burn severity based on the correlation between field-based burn severity indices and remote sensing indices should account for variations in the conditions of pre- and post-fire vegetation.

As noted by many studies, regression models that are used to determine the relationships between readings of burn severity from remote sensing and field measurements are data- and site-specific and, thus, may not be applied to other sites with different cover types and conditions [155,165,172]. However, compared with linear regression, both Cansler and McKenzie [155] and Hall *et al.* [165] found that exponential and second-order polynomial models calibrated better relationships between field-based CBI and dNBR/RdNBR across different ecoregions of temperate forest and boreal forest in North America, respectively. Hall *et al.* [165] mentioned the possibility of a single, non-linear CBI-dNBR model for estimating burn severity over the western Canadian boreal forests. All these authors suggested that land cover and the stratification of similar ecological areas should be applied to improve the prediction of burn severity over large areas.

As a characteristic of fire and burn severity in permafrost regions, the consumption of the organic layer's depth is the most important effect on how a post-fire ecosystem functions in boreal forest [14,66,74]. Some studies suggested that approaches based on remote sensing bands and indices were unreliable, that they mapped fire and burn severity inconsistently and were unable to account for the depth of the post-fire organic layer [69,70,166]. These results suggest that new approaches, which include other predictors, such as topography, solar elevation and plant phenology [75,159] into indices based on remote sensing are necessary in order to successfully model fire and burn severity in dynamic boreal regions, such as the Alaskan boreal forests. Consequently, Barrett *et al.* [67] found that the incorporation of topographic position, remote sensing indices related to soil and vegetation properties, the timing of fire events and meteorological data using regression tree models significantly improved the modeling of burn severity in black spruce stands in the Alaskan boreal forest.

Table 5. Summary of studies using remote sensing data for mapping burn severity in boreal regions; NBR, Normalized Burn Ratio; dNBR, Differenced Normalized Burn Ratio; RdNBR, Relative Differenced Normalized Burn Ratio; dNDV, Differenced Normalized Difference Vegetation Index; BCI, Burn Class Index; SRI, Surface Roughness Index; VCI, Vegetation Cover Index; CBI, Composite Burn Index; $\Delta\alpha_0$, post-fire spring albedo change. A differenced index, such as dNBR, is calculated by subtracting the post-fire index from the pre-fire index.

| Study	Boreal Zone	Year of Image	Remote Sensing Approach	Field Based Indices	Results
Bourgeau-Chavez *et al.* [162]	Black spruce, Alaska	1992 (fire in 1990)	ERS-1 SAR backscatter; multiple linear regression	BCI, SRI, VCI	R^2 depends on season: $R^2 = 0.92$ (spring); $R^2 = 0.64-0.78$ (summer); $R^2 = 0.298$ (autumn)
Michalek *et al.* [77]	Black spruce, Alaska	1995 (fire in 1994)	Supervised classification of Landsat TM	Three classes of burn severity from field observation and aerial photo	Three classes of burn severity: light, moderate, severe
Epting *et al.* [76]	Mixed species, Alaska	2001 (fire in 2001)	Landsat TM bands and indices; linear regression	CBI	$R^2 = 0.6$ (highest correlation between NBR and CBI)
Epting and Verbyla [83]	Black and white spruce, Alaska	1988 (fire in 1986)	Decision tree classification of Landsat TM dNBR	Adjusted dNBR threshold from [76]	Three burn severity classes: high (dNBR $\geq$ 620); moderate ($250 \leq$ dNBR ≤ 620); low ($85 \leq$ dNBR ≤ 250)
Sorbel and Allen [171]	Mixed species, Alaska	1999-2002	Landsat TM dNBR; linear regression	CBI	$R^2 = 0.46-0.84$, depending on fire events
Duffy *et al.* [75]	Conifer and broadleaf, Alaska	1994, 1999, 2000, 2002 (24 fires from 1993 to 2002)	Landsat TM NBR; statistical analysis of NBR (ANOVA, variogram)	n/a	Burn severity (represented by NBR) depends on topography and type of vegetation
Allen and Sorbel [71]	Conifer and broadleaf, Alaska	1999–2003 (fires from 1999 to 2002)	Landsat TM dNBR, linear regression	CBI	$R^2 = 0.45-0.88$, depending on fire events

Table 5. *Cont.*

Study	Boreal Zone	Year of Image	Remote Sensing Approach	Field Based Indices	Results
Hall *et al*. [165]	Western Canada	2004, 2005 (fires in 2003 and 2004)	Landsat TM dNBR, linear and non-linear regression	CBI	$R^2 > 0.7$; non-linear model performed better than linear model
Hoy *et al*. [69]	Black spruce, Alaska	2004 (fires in 2004)	Landsat TM/ETM+ bands and indices; linear regression	CBI	Low correlation between the satellite and field measurement of severity; $R^2 = 0.52$ for highest correlation between dNBR and CBI
Murphy *et al*. [70]	Black and white spruce, Alaska	2005 (6 fires in 2003 and 2004)	Landsat TM dNBR, linear regression	CBI	Low correlation between dNBR and CBI; $R^2 = 0.11-0.64$, depending on fire events
Verbyla and Lord [166]	Conifer and broadleaf, Alaska	1985 (fire in 1983)	Landsat TM NBR, linear regression	Post-fire organic soil depth (measured in 2006)	Low correlation between NBR and organic soil depth; average $R^2 = 0.26$ for all sites; $R^2 = 0.65$ for black spruce sites
Barret *et al*. [67]	Black spruce, Alaska	2005 (fire in 2004)	Landsat TM/ETM+ indices and ancillary data for regression tree model	Organic layer depth	Significantly improved efforts to map organic layer depth representing for fire severity; model fit with $R^2 = 0.8$
Soverel *et al*. [138]	Western Canada	2005-2008 (fires from 2005 to 2007)	Landsat TM/ETM+ dNBR and RdNBR	CBI	RdNBR no more effective than dNBR in estimating burn severity, 65.2% and 70.2% classification accuracy, respectively
Soverel *et al*. [168]	Western Canada	2005–2008 (10 fires from 2005–2008)	Landsat TM/ETM+ dNBR; non-linear regression	CBI	Overall model with $R^2 = 0.69$
Jin *et al*. [167]	North American	2001–2009	Classification of MODIS dNBR and albedo change ($\Delta\alpha_0$)	n/a	dNBR and $\Delta\alpha_0$ values between 20%–45%, 45%–75%, >75% percentiles were classified as low, moderate and high severity classes, respectively
Wu *et al*. [170]	Boreal forest, northeastern China	2010 (fire in 2010)	Classification of Landsat TM dNDVI	n/a	Higher dNDVI values indicated higher burn severity
Cai *et al*. [169]	Boreal forest, northeastern China	2000 (fire in 2000)	Classification of Landsat TM dNBR (3 months after fire) to study tree recruitment 11 years after fire	n/a	High severity: dNBR $\geq$ 743; low severity: dNBR < 743

The stratification of the conditions of pre- and post-fire vegetation, as well as the inclusion of different predictors related to the environment are necessary when mapping burn severity using remote sensing approaches (Figure 3), which is now possible through the development of remote sensing capabilities. Such capabilities, for example, include the classification of Landsat or MODIS imagery for vegetation properties [93], the ASTER digital elevation model for topography [173] and the MODIS active fire and/or AVHRR products for fire regimes [7]. Additionally, all the above characteristics of fire and burn severity have been very well documented in the boreal regions of North

America. However, to the best of our knowledge, there have been no similar studies conducted in other boreal regions, such as Eurasian boreal forests. Because the types of fire and vegetation properties are quite different from boreal forests in North America and Russia [7], similar patterns of burn severity may not be found among these boreal regions. Therefore, these approaches and suggestions require interpolating and validating for boreal forest regions around the world to improve the modeling of burn severity using remote sensing (Figure 3).

Figure 3. Summary of field-based and remote sensing-based measurements of burn severity along with potential challenges and gaps in research in boreal forest ecosystems; LAI, Leaf Area Index; SAVI, Soil Adjusted Vegetation Index; dSAVI, Differenced Soil Adjusted Vegetation Index.
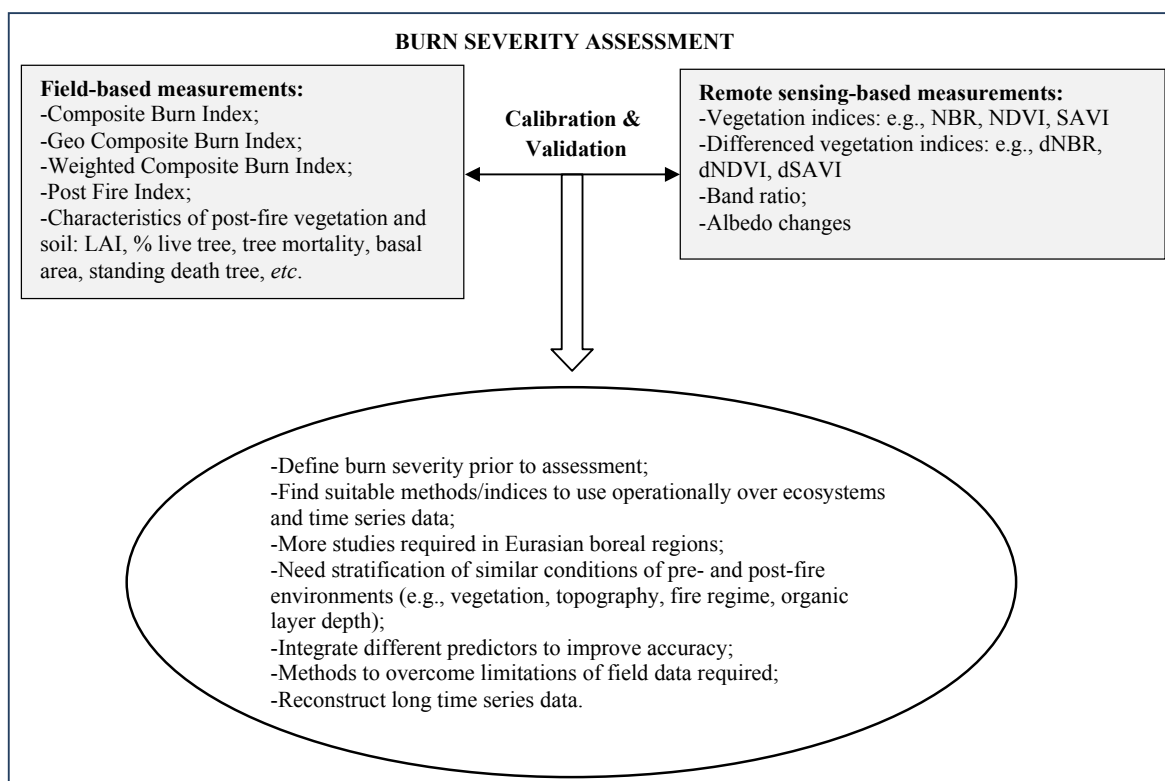
3.2.3. Classification of Remotely Sensed Data to Burn Severity Classes

Even though field-based indices, such as CBI and GeoCBI, and spectral indices, such as NBR, dNBR and RdNBR, are the most widely adopted combination in the investigation of burn severity, they are not yet standard methods for evaluating burn severity in either the remote sensing or fire science communities [21,160]. The assessment of burn severity from both *in situ* and remotely sensed data is also not always available. As a result, there are a variety of methods beyond the models of CBI and vegetation regression indices to evaluate burn severity using remote sensing data, and the results differ widely. For example, percentile classifications of MODIS dNBR and the change of spring albedo ($\Delta\alpha_0$) were employed by Jin *et al.* [167] to assign classes of low (20%–45% percentile), moderate (45%–75% percentile) and high (>75% percentile) severity in North American post-fire boreal forests. The authors mentioned that an alternative approach to measuring burn severity is to

monitor the change in spring albedo, since it depends on the mortality and recovery rate of post-fire vegetation. Epting and Verbyla [83] applied similar Landsat dNBR threshold values (90, 275 and 680), calculated by Epting *et al*. [76], to classify low, moderate and high classes of burn severity in their Alaskan boreal forest study site. However, Cai *et al*. [169] evaluated burn severity in Chinese boreal forests according to the histogram of dNBR values with high severity (dNBR ≥ 743) and low severity (dNBR < 743). All these results confirmed that the above proposed indices, spectral thresholds and methods of assessing burn severity can possibly be adjusted to local conditions, but it is not clear whether they can be extended to other study sites.

It is strongly recommended in the reviews by Lentile *et al*. [20] and French *et al*. [21] that researchers should properly define the need for the assessment of burn severity and clarify the amount of presumption in the methods for measuring burn severity (Figure 3). For example, Boer *et al*. [164] defined burn severity in the southwestern Australian forest as a fire-induced change in LAI (dLAI), since LAI is a clear indicator of the attributes of biophysical vegetation that can be objectively measured in the field. Boer *et al*. [164] concluded that simulating remotely sensed indices, such as NBR, NDVI and the simple ratio, with well-defined biophysical attributes like LAI, is a very objective and rapid way to measure and interpret post-fire effects within the context of fire and forest management. Thus, these assumptions would be alternatives to assessing burn severity based on CBI and GeoCBI, especially for areas with significant gaps in field-based data of burn severity, as well as the areas with a low correlation between CBI and remote sensing indices alone, like the Alaskan boreal forest. However, there is still a need to assess how such methods work with the wide range of environments that are affected by fires in regions of boreal forest (Figure 3). Finally, in addition to the long-time series of burned areas, the long-time series of burn severity is also necessary to characterize vegetation's response to fire under different climatic conditions, but very few studies in the literature have attempted to reconstruct this in either boreal forests or other ecosystems. One example was presented by Sunderman *et al*. [174], who applied Landsat-dNBR thresholds to reconstruct fire severity for a 28-yr period in temperate regions. Some field-based and remote sensing-based indices, as well as some challenges and gaps in research for mapping burn severity in boreal regions, were summarized in Figure 3.

3.3. Remote Sensing-Based Assessment of Post-Fire Forest Patterns

Much of the work described above entails mapping the location, size and severity of disturbance by forest fire. However, the causes and consequences of spatial variability in post-fire effects become increasingly significant to our understanding of how forest ecosystems respond. The spatial variability of post-fire forests can be characterized by stages of forest succession, forest structure and the regrowth of forest composition since disturbance. Remote sensing of disturbances for the express purpose of quantifying forest patterns enables the extraction of independent variables to predict dependent variables, such as successional stages, stand age, tree diameter and height, biomass, canopy closure, species diversity and other structural parameters over large areas of post-fire forest. The overall review of remote sensing in monitoring the recovery of post-fire vegetation in nature was conducted by Gitas *et al*. [175], and remote sensing of the biophysical parameters of boreal forests was conducted by Lutz *et al*. [176]. The review by Gitas *et al*. [175] discussed remote sensing studies of monitoring post-fire vegetation in general, including tropical, temperate, Mediterranean and boreal

ecosystems, while Lutz *et al*. [176] did not focus on studies about monitoring post-fire effects and recovery patterns of boreal forests. Therefore, this section is largely focused on remotely sensed data and methods for monitoring post-fire forest patterns, including successional stages, the attributes of forest structure and the trajectories of forest recovery in regions of post-fire boreal forest. This review will also discuss the data and methods from other ecosystems that can be potentially applied to help understand boreal forest patterns following fire disturbance.

3.3.1. Monitoring Successional Stages

Forest succession is an important ecological process that determines the biophysical, biological and biogeochemical characteristics of forest ecosystems [177]. Patterns of forest succession vary among fire perimeters depending on many factors, such as site conditions before and after a fire, the extent of the fire and the severity of the fire. In boreal larch forest ecosystems, the size and severity of fires, coupled with climatic condition, are among the principal factors influencing post-fire dynamics and patterns of succession [82,178]. For example, three classes of forest successions were determined after climate change and fire in the taiga larch forest in central Siberia, including succession with no replacement of tree species, succession with replacement of a tree species and succession with open larch stands replaced by shrubby tundra [82]. Furthermore, the length of complete stages of succession in Siberian boreal forests strongly depends on fire intervals and species characteristics, ranging from five years as the first stage of succession, in which pine regenerates successfully, to more than 180 yr as the last stage of succession, represented by old pine stands [82], and from two years to 90 yr as the first and last stages of succession in larch stands, respectively [9]. Similarly, the influences of fire severity on the succession of the Siberian larch forest illustrates that during a surface fire with low severity, conditions of pre-fire vegetation can recover after 5–8 yr, while the dominant, pre-fire trees are restored within 7–15 yr and 15–20 yr after moderate and high larch fire severity, respectively [179]. Pioneer species of herbs and grasses are dominant in the larch forest during the first four years after high fire severity [179]. Through the periodic measurement of post-fire tree density over several decades, Johnstone *et al*. [180] found that North American boreal tree recruitment occurs within a short (3–10 yr) period after fires. Additionally, the observation of patterns of stand density and composition within five years after fires can be used to predict forest patterns observed two or three decades after fires [180].

The identification and classification of the successional stages of forests over large areas are challenging to conduct based on field surveys alone. Combining field plots with remotely sensed data, however, provides an alternative approach for monitoring successional stages of forests across large spatial extents [177] (Table 6, [83,177,181–186]). In boreal forest ecosystems, there are very few studies using optical sensors, such as Landsat TM/ETM+, to characterize post-fire patterns of succession [83,187–189]. One known study of burn severity and post-fire succession through remote sensing was conducted by Epting and Verbyla [83] over a 16-yr post-fire period in interior Alaska. Landsat TM/ETM+ images were used to categorize two successional classes of self-replacement and relay floristic with respect to burn severity and pre-fire vegetation. In this study, both pre- and post-fire images were classified using an unsupervised method of classification to identify six types of vegetation, including closed needle-leaf forest, open needle-leaf forest, needle-leaf woodland,

broadleaf forest, mixed forest and shrub land. The strategy for monitoring successional stages by Epting and Verbyla relied on a similar approach with change detection using post-classification maps. Pixels exhibiting the same class of vegetation in both pre- and post-fire images were classified as self-replacement succession, whereas areas that changed classes of vegetation from spruce-dominated to broadleaf-dominated were classified as relay floristic areas [83]. The result showed that post-fire patterns of succession in Alaskan boreal forests strongly depended on the types of pre-fire vegetation and burn severity. For example, most of the high burn severity areas with closed needle-leaf, open needle-leaf and mixed forest classes shifted to woodland or shrubland, sixteen years after the fire [83]. However, Epting and Verbyla noted that the study only focused on one burn in the late growing season and that the result may not represent patterns of burn severity and the succession of post-fire vegetation across the Alaskan boreal region. Discrimination of spectral bands and vegetation indices by Landsat TM/ETM+ imagery has been the more commonly used approach to identify the distribution of successional forest stages in temperate regions, compared with boreal regions [177,181,190–193]. Song *et al*. [181] demonstrated that the temperate conifer forest's successional stages can be differentiated using a linear regression analysis between the Landsat Tasseled Cap classes of brightness, greenness and stand age. Liu *et al*. [177] found that using forest inventory plot data and Tasseled Cap with two other predictive models, such as decision trees and neural networks, were more successful than linear regression models in predicting a forest's successional stages. This is due to the fact that these models are not necessary data with normal distributions, and they can eliminate the spectral noise of forest samples. Both Song *et al*. [181] and Liu *et al*. [177] used a chronosequence approach that substitutes space for time, and they concluded that multi-temporal Landsat imagery clearly improved the discrimination of young, mature and old temperate forest stands. This is due to the fact that multi-temporal data can take advantage of annual phenology to improve the classification of different successional stages and pathways [182]. With the different coverage and the availability of Landsat data from 1972 to the present at local-to-continental scales, these multispectral data are valuable for producing classifications of stages of forest succession at these different scales (Table 6).

In addition to optical sensors, LiDAR (Light Detection and Ranging) imagery has proven particularly useful to estimate forest structures, as well as to characterize stages of forest succession, since LiDAR measures the three-dimensional arrangement of forest canopies. In Eurasian boreal forests, LiDAR data have been used to separate different types of forest sites in general, ranging from poor (xeric heath forest) to very rich forest [184], and to identify stands of boreal forests with high herbaceous plant diversity [185]. As mentioned by Falkowski *et al*. [186], that classifications of forest succession should reflect all potential stages of forest development, the authors successfully used LiDAR height metrics to classify six stages of forest succession across a structurally diverse and mixed-species conifer forest. Six stages of succession were characterized using LiDAR data in conjunction with a non-parametric Random Forest algorithm, resulting in an accuracy greater than 95% overall. The use of nonparametrics, such as the Random Forest classification algorithm, can incorporate a number of continuous and categorical predictors, develop robust predictions and account for uncertainty when mapping successional classes [186,194]. The LiDAR-based techniques of data analysis are applicable to the detection of different post-fire stages of succession in boreal forests, because of specifically slow recovery rates of boreal tree saplings combined with extensive shrub

regrowth for the first several decades following fires in boreal forests. However, it is noted by Falkowski *et al*. [186] that LiDAR data is associated with very high costs for mapping at regional and continental scales and is not available at all footprints [186]. To our knowledge, there have been no similar studies, either in general or in sites specific to post-fire environments, conducted in boreal regions to identify *all* potential successional stages using LiDAR imagery. A similar approach to Falkowski *et al*. [186] can be conducted to develop and evaluate methods for mapping post-fire forest succession in boreal forest ecosystems (Table 6).

Spaceborne synthetic aperture radar (SAR) data also provides an alternative approach for monitoring the regrowth of post-fire forests, since backscatter is also sensitive to forest structural parameters. The backscatter coefficient typically increases with forest biomass, and SAR wavelengths are able to differentiate among grass, shrub, young and mature forest stands [195], commonly represented in secondary forests following fires. Based on the advantage of SAR cross-polarized backscatter, which is more sensitive to forest structure and different stages of forest regrowth, Tanase *et al*. [183] used X-, C- and L-band cross-polarized backscatter to monitor forest regrowth in both Mediterranean and boreal forests affected by fires. The authors found that up to four different stages of post-fire regrowth in boreal forest could be distinguished, whereas five phases of regrowth in Mediterranean forests were discerned using L-band SAR data. However, compared with the NDVI from optical sensor, the reliable differentiation of regrowth phases using NDVI could only be observed for the most recent stages of development (10–20 yr after disturbance), because NDVI responded positively to changes in canopy recovery and then saturated prior to the point where an ecosystem fully recovers from disturbance [183]. These results suggest the usefulness of SAR data for monitoring forest regrowth after disturbances. However, Kasischke *et al*. [196] reported that L-band microwave backscatter was the most sensitive to variations in aboveground biomass and soil moisture in boreal forests. More specifically, soil moisture did significantly change the correlation between the L-band backscatter and the aboveground biomass typically found in boreal forests that are regenerating, and the influence of soil moisture is dependent on the biomass [196]. Therefore, the consideration of soil moisture conditions over the study area is important when using SAR backscatter to monitor post-fire forest regrowth and forest structure [183,196] (Table 6).

Generally, the classification of forest successional stages is different from the types of land cover classification, as forest succession involves ecological processes and requires viewing the vegetation community as a continuum rather than as discrete classes [184,197,198]. Classification of forest succession, therefore, not only benefits sustainable forest management, but also effectively quantifies ecological responses and relationships in wildlife habitats [199,200]. Additional studies should be performed on whether optical remote sensing data and methods can be confidently applied to monitor post-fire succession of boreal ecosystems, since these data can be archived, historically corresponding to each stage of forest succession. Optical remote sensing data, such as Landsat, AVHRR and MODIS imagery, are also freely accessible online. The capabilities of remote sensing data and methods often used in the literature to identify successional stages in boreal forests and other regions were summarized in Table 6 as follows.

Table 6. Selection of data and methods commonly used for mapping successional stages in boreal forests and other regions. Selected studies were found in both Alaskan (e.g., Epting and Verbyla [83] and Tanase *et al.* [183]) and Eurasian (e.g., Vehmas *et al.* [185] and Vehmas *et al.* [184]) boreal regions. However, studies conducted in Eurasia are not specific to post-fire recovery sites. Therefore, conducting more studies in this region is required. LiDAR, Light Detection and Ranging.

Data	Method	Identified Stage	Advantage	Disadvantage	Selected Study
Optical sensor: Landsat TM/ETM+	-Chronosequence approach; -Supervised/unsupervised classification; -Linear regression of spectral bands/indices (e.g., NDVI, Tasseled Caps) and stand age classes; -Non-parametric methods (e.g., decision trees and neural networks)	-Identified different stages of forest succession, such as young, mature and old forest; or self-replacement and relay floristic	-Multi-temporal data can represent annual phenology to improve discrimination of successional stages; -Available to classify forest successional stages at regional-to-continental scales	-Limited in measuring three-dimensional structural attributes related to forest succession; -Limited in identifying some understory successional classes, since the overstory canopy blocks the understory signal; -Insignificant spectral signature response to low regrowth rate and unreliable differentiation of mature and old regrowth phases due to the saturation of the spectral signature (e.g., NDVI)	[83,177,181–183]
LiDAR: LiDAR pulse height metrics	-Chronosequence approach; -Non-parametric methods (e.g., logistic regression and random forest algorithm): LiDAR metrics used as independent predictors	-Identified all potential stages of forest stand development, such as open stem, stand initiation, understory initiation, young multistory, mature multistory and old multistory	-Incorporated three-dimensional structural attributes to accurately monitor different vegetation growth stages; -Able to capture a broad range of vegetation characteristics in a consistent and transparent manner; -Unaffected by solar illumination and visibility (e.g., clouds);	-Limited in differentiating seedling and saplings (first stages of forest formation) from other understory components; -Still influenced by very dense canopy forests that limits direct characterization of understory components and species (canopy penetration); -Currently limited in mapping forest succession at regional to continental scales due to small footprint and high cost;	[184–186]

Table 6. *Cont.*

Data	Method	Identified Stage	Advantage	Disadvantage	Selected Study
SAR: Cross-polarized and co-polarized backscatter	-Chronosequence approach; -Descriptive statistics, analysis of variance (ANOVA) and pair-wise comparison to discern between forest recovery stages using SAR backscatter and coherence; -Linear and non-linear regression models	-Differentiated regrowth phases, such as undisturbed forest, young, mature and old forest; or by stand age: 20–40 yr, 15–20 yr and <15 yr	-Taking advantages of L-band backscatter sensitivity to forest structural parameters allowed the differentiation among young, mature and old forest stands; -Unaffected by solar illumination and visibility (e.g., clouds); -Able to monitor forest succession over regional and continental scales	-Sensitivity of backscatter to soil moisture required the development of approaches to account for variations in soil moisture avoiding the misclassification of regrowth stages; -Limited in differentiating understory classes and early successional stages (e.g., areas with forest regrowth from recent disturbance) from other components; -Co-polarized repeat-pass coherence can only separate regrowth phases for the most recently affected sites (<15 yr since disturbance) regardless of the radar frequency	[183]

3.3.2. Measurement of Other Variables in Forest Structure

The structural attributes referring to the spatial arrangement and distribution of a forest are important surrogates to indicate the functional and compositional attributes of forests. The structural attributes used to characterize forest patterns, including successional stages, can be grouped into three main categories: (1) attributes of biophysical and spatial distribution, such as Leaf Area Index (LAI), crown closure/canopy cover, breast height diameter (DBH), height, basal area, volume or biomass, stem/seedling density and stem age/stage of development; (2) species diversity represented by diversity indices, such as the Shannon–Weiner and Simpson indices; and (3) complexity of forest structure (SCI) comprising variations of different spatial attributes, such as DBH, height, basal area and age [78,79,197,201]. Since post-fire forest environments and forest patterns are significantly different from pre-fire environments, the review of this section will focus more on remote sensing data and methods that have been applied to monitor structural parameters following disturbances in boreal forests. Some studies in other forest ecosystems and undisturbed environments that might be useful for measuring variables in post-fire boreal forests were also included and discussed in this review.

Applications of remote sensing aimed at monitoring structural attributes of forests that were listed above have been driven largely by using empirical models to calibrate remotely sensed data with *in situ* data in either boreal or other forest ecosystems (Table 7, [8,28,112,187,196,202–213]). For example, regression-based prediction has been a widely accepted approach to mapping regional forest attributes using linear regression [196,203,204,213], nonlinear regression [187,209‑211,214,215], partial least squares regression [216] and regression tree algorithms [26,217]. Recently, non-parametric regression

approaches, such as Reduced Major Axis (RMA) regression, k-Nearest Neighbor (k-NN), Gradient Nearest Neighbor (GNN) and Random Forest (RF) regressions, have received considerable attention for the estimation of structural forest attributes, because these approaches can account for mapping uncertainty and involve a large number of response variables with analytical and operational flexibility [28,209,218].

Many studies have demonstrated that correlation between independent bands/indices of optical imagery and dependent, site-based forest biophysical variables have a high variation, depending upon derived variables, spectral bands/indices, vegetation properties and disturbance regimes. In post-fire Canadian boreal forest, Zhang *et al.* [187] modeled stand age distribution using a Shortwave Vegetation Index (SWVI) calculated from SPOT VEGETATION imagery. The dated fire scars were based on historic fire data, and the stand age was by pixels of each type of land cover since the fire derived based on the polynomial relationship between stand age and the mean SWVI, with the highest correlation for the mixed coniferous forest ($R^2 = 0.53$) [187]. However, the result showed that using SWVI to estimate stand age was limited due to systematic bias with an overestimation of the stand age of about five years for young stands and an underestimation of up to 15 yr for old stands. This index also saturated at different points, depending on the types of land cover and the number of years since the fire. For example, the SWVI of coniferous forests saturated at the value of about 0.25 after 37–42 yr since the fire, while the saturated value of deciduous forest was 0.35 at a post-fire regeneration age less than 10 yr. These findings were similar to Fraser and Li's [112] based on a sample of fires across Canada. Fraser and Li [112] also found that an artificial neural network (ANN) model performed better than multiple regression in predicting the age of regenerating boreal forests after fire. Both studies mentioned that an understanding of burn severity and the spatial heterogeneity of fire disturbance will improve the prediction of forest stand age regenerating after fire with a high level of accuracy. Similarly, some studies were conducted in Siberian boreal regions to monitor forest variables after fires using a moderate resolution dataset [202,205,219]. For example, Chen *et al.* [202] validated the collection 4 MODIS LAI product (MOD15) and Landsat ETM+-derived LAI in different post-fire sites and found that the MODIS LAI product correctly represented the summer site phonologies, but significantly underestimated the LAI value of the site, with a 100-year-old post-fire deciduous forest during the winter period. Compared with the Landsat ETM+-derived LAI, the MODIS LAI overestimated values in the low LAI deciduous forests (LAI < 5) and underestimated values in the high LAI conifer forests (LAI > 6). Additionally, the Landsat ETM+-reduced simple ratio (RSR) significantly improved the LAI prediction, while the Enhanced Vegetation Index (EVI) had the poorest performance in the estimating LAI ($R^2 = 0.89$ and $R^2 = 0.61$, respectively). Because of the high variation of the MODIS LAI product, further comparison with field datasets and other LAI products (e.g., CYCLOPES LAI product [205]) from other boreal forest sites is necessary to improve LAI quantification in disturbed forest landscapes.

Table 7. Some common remote sensing approaches used to estimate post-fire forest patterns in boreal regions; RSR, Reduced Simple Ratio [202]; SWVI, Shortwave Vegetation Index; GLAS, Geoscience Laser Altimetry System on ICESAT. Other examples of remote sensing approaches for monitoring forest structure in undisturbed boreal forests, as well as other post-fire forest ecosystems can be found in [8,28,203–207].

Satellite/Sensor	Independent Variable	Derived Forest Parameter	Method	Result/Accuracy	Study
Landsat TM/ETM+	NDVI, EVI and RSR	LAI	Linear regression models	$R^2 = 0.61$ and $R^2 = 0.69$ for EVI and NDVI model, respectively; $R^2 = 0.89$ for the RSR model	[202]
SPOT VEGETATION	SWVI and NDVI	Stand age	Non-linear regression and artificial neural network	$R^2 = 0.29{-}0.53$; RMSE < 10 yr	[112,187]
MODIS	MODIS LAI	LAI	Compared with field-based LAI and the finer resolution data of LAI (Landsat ETM+)	Overestimated in the low LAI (LAI < 5); underestimated in the high LAI (LAI > 6)	[202]
LiDAR (airborne and spaceborne-GLAS)	Year since fire	Canopy height	Forward-stepwise regression	$R^2 = 0.78$	[208]
	Airborne LiDAR height metrics	Canopy height, vegetation fill, crown closure, volume and total biomass	Subtracting the ground surface elevation profile from corresponding LiDAR measurements for canopy attributes; empirical model for volume	$R^2 = 0.73{-}0.8$ for volume estimates from canopy profile area; relative standard error of 7.3% for total biomass estimate	[209–211]
LiDAR (airborne and spaceborne-GLAS)	Spaceborne (GLAS) LiDAR height metric	Average tree height	Linear regression	$R^2 = 0.74$ (RMSE = 5.7 m)	[212]
SAR	C-band backscatter	Soil moisture	Linear and polynomial regressions; principle component analysis	$R^2 = 0.56{-}0.82$ (RMSE = 3.61)	[213]
	L-band backscatter	Aboveground biomass	Linear regression	$R^2 = 0.49{-}0.63$ (RMSE = 2.8–3.3 t/ha)	[196]
LiDAR + Landsat/MODIS	LiDAR height metrics and Landsat-derived layers (e.g., land cover and burn severity)	Canopy/tree height, vegetation fill, crown closure, volume, and total biomass	Linear regression between forest attributes derived from LiDAR and spectral indices; stratifying canopy height at different burn severity	Spatially explicit identifications of forest regrowth; Strong positive correlation between post-fire conditions (burn severity and forest type) and canopy attributes ($R^2 = 0.5{-}0.7$)	[210–212]
LiDAR + SAR + Landsat	LiDAR height metrics, SAR backscatter and Landsat TM bands	Aboveground biomass	k-NN nearest-neighbor imputation to predict biomass within each grid cell, using LiDAR grid cells as the reference data and the Landsat/SAR data as the target data	Substantial improvement of standard error from 7.3% to 5.1% with the inclusion of Landsat and SAR data	[209]

Similar to mapping forest succession, some studies mentioned that the inclusion of derived spectral indices, raw spectral bands, biophysical variables and time series data can improve the estimation of structural attributes of post-fire forests. Li *et al*. [217] used Landsat TM and ETM+ to model the height of young forests after fire disturbances in Mississippi, USA, and found that the inclusion of modeled stand age, Landsat raw bands and vegetation indices, such as forestness index (FI), NDVI and NBR, as predictors significantly improved model error over those based only on spectral models, especially with regression tree models rather than step-wise linear regression models. Pflugmacher *et al*. [206] found that live forest biomass estimated by using Landsat time series (LTS) data was of much higher accuracy than that by single-date Landsat data, and LTS models for the estimation of dead biomass above ground performed significantly better than those with either LiDAR data or single-date Landsat data. This suggests that long-term LTS metrics can reveal not only disturbance events, but also recovery progress that directly relates to current forest structure and, thus, finally, improved estimation of current structural attributes of forests. To our knowledge, there has been no evidence in the literature considering those approaches with optical sensors to determine structural attributes in boreal forests following fires.

In addition to optical sensors, a number of studies have been conducted in boreal regions to determine the structural attributes of boreal forests using LiDAR and SAR data (Table 7). For example, Kasischke *et al*. [196] investigated the use of L-band SAR data for estimating aboveground biomass in post-fire Alaskan boreal forest sites and found that the backscatter from SAR data was a reliable predictor for estimating aboveground biomass using a linear model, especially in the area with highest soil moisture (R^2 = 0.63, RMSE = 3.2 t/ha). The results suggested that the estimation of biomass in post-fire biomes using L-band SAR should account for variations in soil moisture, since soil moisture did change the correlation between L-band microwave backscatter and aboveground biomass in sites with a low level of vegetation regrowth [196]. Additionally, Magnussen and Wulder [208] assumed that post-fire forest patterns are typically composed of both post-fire regeneration and elements of pre-fire vegetation, so that the measurement of post-fire structural attributes requires a separation of the burned and unburned structural elements. Consequently, Magnussen and Wulder [208] successfully separated post-fire and recovered canopy heights from pre-fire canopy heights in Canada's boreal forests using a sequential statistical procedure with LiDAR data. The study also indicated that the mean regenerated post-fire canopy heights had a positive high correlation with the number of years since the fire.

Although airborne LiDAR and SAR data have been successfully used to derive structural attributes of vegetation, an alternative approach to mapping forest attributes is to use these measurements in combination with remotely sensed optical imagery [207,209–212,220]. This synergistic use of active and passive sensors provides opportunities to fully characterize the structural attributes and dynamics of forests with regard to disturbance regimes (e.g., burn severity) and pre- and post-fire vegetation types (Table 7). Wulder *et al*. [210] demonstrated that the overall trend in changes of forest attributes derived from airborne LiDAR height profiles were stable during a five-year period in Canada's boreal forests without segmented spectral information from Landsat imagery. On the other hand, a local approach for measuring changes in forest attributes over time, using spectrally homogeneous segments derived from Landsat ETM+ data to stratify the LiDAR transect, showed explicit indications of spatial forest growth and depletion. The difference in the magnitude of the changes was greater for degradation, but was less extensive spatially than it was for growth [210]. Wulder *et al*. [210]

suggested that a local approach was more appropriate for characterizing the heterogeneity of dynamic forest ecosystems over broad areas, due to the fact that growth tends to occur incrementally over broad areas, whereas degradations are dramatic and are constrained spatially. Regarding the relationship between post-fire conditions and post-fire forest structure, Wulder *et al*. [211] analyzed forest structure, derived from airborne LiDAR height metrics, and post-fire conditions, as measured in burn severity from Landsat data, and found that the structural attributes of post-fire forests were strongly correlated to post-fire NBR, dNBR and RdNBR. However, there were no marked differences in the performance of post-fire NBR, dNBR and RdNBR for characterizing post-fire effects. The relationship between post-fire structure and post-fire condition was strongly dependent on the types of post-fire vegetation [211]. These findings were consistent with a recent study by Goetz *et al*. [212] that explored post-fire canopy height in Alaska using the integration of spaceborne LiDAR, MODIS and Landsat imagery. Goetz *et al*. [212] suggested that the consideration of post-fire conditions derived from optical imagery, such as burn severity and types of regenerated vegetation, was important for modeling forest regrowth using spaceborne LiDAR height metrics data acquired from the Geoscience Laser Altimetry System (GLAS) on ICESAT. Similarly, Andersen *et al*. [209] also found that the integration of Landsat TM, LiDAR and SAR data improved significantly in the precision of estimating total biomass in the boreal forests of interior Alaska via nearest-neighbor imputation over the single use of LiDAR data modeling (reduction in relative standard error from 7.3% to 5.1%). This is probably because the inclusion of both spectral and L-band SAR backscatter provided information that contained the two most important attributes of three-dimensional forest structure and species composition in quantifying aboveground biomass [209].

In general, regarding remote sensing data and methods for modeling forest variables, Powel *et al*. [28] assumed that it is difficult to conclude outright that one modeling technique outperforms the other. The performance of each method depends on measures and scales of validation. As a result of disturbances, the prediction of a forest's structural parameters also depends upon the nature and level of the disturbances, and so, linkage with accurate maps of forest disturbance might provide a more reliable interpretation of variations in forest structure relative to the process of disturbance and regrowth. In the case of approaches using remote sensing for monitoring boreal forest variables following fire disturbance, this suggests that stratification of post-fire conditions and the inclusion of disturbance regimes, such as fire frequency, burned area and fire/burn severity [211,212], in modeling post-fire forest patterns might have the potential to improve the accuracy and interpretation of models.

3.3.3. Tracking Patterns of Forest Recovery after Fire

Remote sensing with time series data offers considerable potential in the trajectory of post-fire forest dynamics, beyond monitoring forest succession and current structural attributes of forests after fires. Many studies have addressed this issue by using moderate-to-low resolution time series NDVI, SAVI, EVI, albedo, NDVI-based Net Primary Productivity (NPP), fraction of absorbed photosynthetically active radiation (fAPAR) and, recently, the vegetation optical depth (VOD) parameter from the Advanced Microwave Scanning Radiometer for Earth Observing System (EOS) (AMSR-E) sensor as surrogates representing the recovery of vegetation after fire disturbances in both the Siberian boreal forest [219,221] and North American boreal forest [81,83,167,183,208,222–226] (Table 8).

Table 8. Observations of the recovery of post-fire forests using time series vegetation indices in boreal regions. The recovery period is determined by the recovery period of the vegetation index value from the burn year to either its maximum value or its pre-fire value, depending on the study; VOD, Vegetation Optical Depth parameter from NASA; AMSR-E, Advanced Microwave Scanning Radiometer for EOS sensor; fAPAR, fraction of absorbed photosynthetically active radiation; NDSWIR, Normalized Difference Shortwave Infrared Index.

Boreal Zone	Sensor/Resolution	Index/Method	Recovery Period	Reference
Alaska/white and black spruce	AVHRR (1.1 km)	NDVI	Maximum at 25 yr for black spruce; 50 yr for white spruce following a fire	[222]
Alaska	Landsat TM/ETM+ (30 m)	NDVI, NBR	8–14 yr for NDVI recovery to the pre-burn level	[83]
Alaska	MODIS	Albedo, EVI and Simple Ratio (SR); time series and chronosequence approach	Maximum of summer albedo, EVI and SR at 25–30 yr since fire	[223,224]
Alaska	SAR	L-band backscatter; chronosequence approach	Recovery of L-band backscatter at burn sites to the backscatter level of undisturbed forests after 60 yr since fire	[183]
Canada	AVHRR PAL (8 km)	NPP/NDVI	About 9 yr for NPP recovery to the pre-burn level	[81]
Canada	AVHRR GIMMS and AVHRR PAL (8 km)	NDVI	>5 yr for NDVI recovery to pre-burn level	[225]
Canada	MODIS (1 km)	Albedo, EVI (monitoring changes in early succession only)	Summer albedo and EVI significantly increase for the first 8 yr after fire	[167]
North America (Alaska and Canada)	AMSR-E (25 km)	VOD	3–7 yr since the fire for VOD to recover fully	[226]
Canada	LiDAR	LiDAR canopy height	Increased trend of canopy metrics for 60 yr since fire	[208]
Siberia	MODIS (1 km)	fAPAR	Very little change of fAPAR in the first 3 yr following a fire	[219]
Siberia	MODIS (1 km)	NDVI, NDSWIR	More than 13 yr since fire for NDVI and NDSWIR to recover fully	[221]

With respect to the post-fire recovery of NDVI [83,221,222,225,227], Normalized Difference Shortwave Infrared Index (NDSWIR) [221], NDVI-based NPP [81] and fAPAR [219], the observations of the recovery of vegetation from these analyses varied greatly, even in the same eco-region, depending upon data resolution, pre-burn vegetation, burn severity and the temporal and spatial variability of vegetation indices within burned and unburned areas (Table 8). Kasischke and French [222] used AVHRR-NDVI time series spanning over three years (1990–1992) to study 14 test sites in Alaska and found that patterns of forest recovery were defined by pre-fire vegetation and the timing of the wildfire during the growing season. The authors found that NDVI increased and reached

its maximum after 20–50 yr using the chronosequence approach to observe post-fire succession of three different types of vegetation, since fires depending on species following fires, followed by a decline of NDVI values. Goetz *et al.* [225] used two NDVI time series derived from the Pathfinder AVHRR Land (PAL) and the Global Inventory Modeling and Mapping Studies (GIMMS) AVHRR to investigate the recovery of vegetation after fires in the boreal forests of Canada. Their results indicated that the recovery rates based on NDVI of Canadian boreal forest were different between the PAL and GIMMS datasets, but both were consistently shorter than previous studies, e.g., [81,222]. This is probably because the previous studies in North America only emphasized the most impacted pixels within fire perimeters [225], which might require a longer period to return to pre-fire conditions [221]. In comparison with North American boreal forest, Cuevas Gonzalez *et al.* [221] found that it took more than 13 yr for the burned Siberian boreal forest to recover fully to pre-fire conditions with respect to NDVI and NDSWIR extracted from MODIS time series data. This recovery rate was longer than the five-year recovery period reported by Goetz *et al.* [225] and the four-year period investigated by Hicke *et al.* [81] in North America. Cuevas Gonzalez *et al.* [221] assumed that the differences in fire regimes and fire types, growing conditions, species composition and data resolution between the Siberian and North American studies might have influenced these results. Similarly, Alcaraz-Segura *et al.* [227] also mentioned that the low resolution data processing (1–8 km observation), such as GIMMS-NDVI data, may introduce a bias that tends to underestimate positive NDVI trends in the Canadian boreal forest.

Surface albedo increases dramatically throughout the first decade after a fire due to the establishment and growth of grasses, shrubs and deciduous broadleaf trees [224]. Since tree canopies establish and typically succeed from broadleaf to conifer species in boreal forest ecosystems, post-fire forest recovery gradually decreases albedo [180]. Therefore, monitoring the change in albedo during vegetation's recovery period following fire could be an alternative approach to determine the effects of fire on post-fire environments and also to understand the trends of vegetation recovery. Jin *et al.* [167] used MODIS data to derive burn severity, albedo and vegetation productivity and then analyzed the dynamics of the recovery of vegetation and albedo during the early stages of succession in Canadian boreal forests. They found that in spring and summer, the albedo increased during the first seven years after the fire and reached higher than the pre-fire level, with the larger increase of post-fire albedo in the site with higher burn severity. These changes of post-fire albedo followed consistently with both EVI changes that recovered to a pre-fire level for 5–8 yr after the fires depending on burn severity classes [167] and NDVI changes that were often higher than pre-fire levels between five to 15 yr after fires across Canada [225]. Compared with the result reported by Beck *et al.* [223], Jin *et al.* [167] assumed that spring and summer albedos following fires increase consistently with the development of stand age from early stages of succession to intermediate-aged stands. However, further studies are needed to assess and understand the inter-relationship between albedo change under the impact of fire and the stages of development in post-fire stands, with the inclusion of species composition, forest structural attributes, burn severity and vegetation productivity. A key challenge in this regard might be to quantify the change in magnitude and directionality of albedo and surface energy across successional stages and gradients of burn severity.

Vegetation indices and products derived from them have been the most frequently used tool for monitoring, analyzing and mapping the temporal and spatial dynamics of post-fire environments.

However, these remotely sensed data, NDVI for example, usually reach saturation levels prior to the point where an ecosystem fully recovers its maximum biomass after disturbance [204,225,228] (Table 9). Therefore, tracking recovery patterns in vegetation using vegetation indices might limit and underestimate the rate of recovery after disturbance [183]. Similar to measuring a forest's structural attributes and successional stages, SAR and LiDAR data have the potential to track the rate of a forest's recovery following disturbance [183,208], since the signal from these data is sensitive and varied by the forest structure and stages of development [184,195] (Table 8). Magnussen and Wulder [208] used LiDAR pulse returns to estimate post-fire recovery rates measured by the mean growth rate of canopy height per year since the recorded fire, over burned areas in Canada's boreal, forest with acceptable levels of precision. The authors also suggested that monitoring the regrowth of canopy height using airborne laser scanner data requires a separation of the burned and unburned structural elements within the perimeter of the fire. Tanaset *et al.* [183] successfully used SAR images to identify regrowth phases in Mediterranean forests and Alaskan boreal forest. The trajectories of forest recovery as seen by L-band HV SAR in both ecosystems showed that L-band backscatter was a negative response to the forest regrowth [183]. In terms of how the percentage of change following a fire shows the recovery rate, Tanase *et al.* [183] indicated that L-band SAR backscatter provided much longer monitoring intervals of 45–60 yr, compared with the analysis of the NDVI that saturated at about 10–20 yr after disturbance in boreal forest. Since forests may need decades to fully recovery to pre-fire conditions with respect to species composition and forest structure (90 yr for the Siberian larch forest, for example [9]), the longer intervals for monitoring L-band SAR data would be useful for tracking the rate of forest recovery. However, as noted by Kasischke *et al.* [196], using SAR data to measure biophysical parameters of a forest's regrowth will require the development of methods to account for variations in soil moisture, particularly in the Alaskan boreal forest.

Even though many current studies have used optical vegetation indices, such as NDVI, to describe forest recovery after disturbances, according to Frolking *et al.* [229], the assumption that the index of vegetation recovery equates to forest recovery may be inappropriate. Buma [230] examined this hypothesis using MODIS time series data from 2000 to 2010 in the area of burned forest in Colorado's Routt National Forest, USA, and demonstrated that NDVI is poorly correlated with forest recovery represented by seedling density in burned areas. Therefore, studies on post-fire forest recovery should consider the inclusion of structural forest ground variables, such as seedling recruitment, percent of cover, tree diameter and height, directly to remotely sensed parameters [34,175,230] (Table 9). To date, however, very few studies in the literature have attempted to tie post-fire ground variables to remotely sensed data with different metrics and spatial scales in either boreal forests or other ecosystems. One example was presented by Roder *et al.* [52], who derived trajectories in post-fire vegetation change by exponential functions with the estimation of green vegetation cover from 20 Landsat MSS, TM and ETM+ (covering 25 yr). These changes in trajectory were used to describe recovery phases following fires in the Ayora region in eastern Spain. In addition to field-based observations, the evaluation of satellite datasets in monitoring post-fire forest recovery should include comparisons of independent observations at the stage of results, for example, comparing detected trends of different optical datasets [225,227] and optical and SAR/LiDAR datasets in different regions [183]. Finally, as noted by some authors (e.g., [221,222,225,227]), analyzing patterns of vegetation cover in boreal forests using remote sensing data requires the development of approaches to

account for variations in spatial and spectral resolution of remotely sensed data, environmental conditions (e.g., clouds and haze, soil moisture, albedo, latitude, topography, climate), vegetation characteristics (e.g., species composition, land cover type, vegetation phenology) and disturbance regimes (e.g., fire and burn severity, fire type, fire frequency). A useful approach might be the stratification of those factors with similar conditions prior to applying remote sensing tools (Table 9).

Table 9. Some limitations and possible solutions in the monitoring patterns of recovery in post-fire boreal forests.

Limitation/Challenge	Solution	Selected Studies as References
1. Saturation of vegetation indices in monitoring the progress of forest recovery and the recovery of vegetation indices may not equate to actual forest recovery with respect to composition and structure of pre-fire forest	-Remotely sensed calibration and validation data with field observations of forest attributes; -Combination of optical and SAR/LiDAR imagery to account for both forest structure and forest composition in post-fire recovery.	[52,183,209,210,230]
2. Variations in the spatial and spectral resolution of remotely sensed data, environmental conditions, vegetation characteristics and disturbance regimes	-Stratification of different conditions prior to applying remote sensing algorithms; -Application of multi-temporal and multi-sensor data, uncertainty based models (e.g., bootstrap based procedures, geospatial approach)	[28,83,196,208]
3. Diverse results and low accuracy in the prediction models of post-fire forest patterns	-Inclusion of different predictors, such as spectral bands/indices, biophysical and environmental parameters in modeling forest patterns;	[8,177,181,206,209,210,227]
3. Diverse results and low accuracy in the prediction models of post-fire forest patterns	-Inclusion of disturbance regimes, such as fire frequency, burned area and fire/burn severity in model prediction; -Utility of multi-temporal remote sensing imagery to account for temporal variations in forest patterns; -Application of uncertainty-based models to account for the uncertainty of mapping forest patterns; -Exploitation of the potential integration of optical and SAR/LiDAR imagery; -Application of high resolution spatial data, such as IKONOS and QuickBird; -Comparison of results derived from different methods and data	[8,177,181,206,209,210,227]
4. Operational models applied to monitor and reconstruct boreal forest patterns following fires	-Exploitation of different image analysis techniques in order to develop robust, automated and transferable algorithms	-

4. Research Summary and Opportunities

4.1. Limitations and Challenges of Monitoring Post-Fire Effects and Forest Patterns

The influences of fire and climate change generate a wide range of temporal and spatial forest heterogeneity, and hence, the interpretation of fire and climate change effects, causal factors (e.g., fire regimes, soil properties, landforms) and ecological responses are a challenge to both scientists and

managers. As reviewed in the present paper, remote sensing has great potential applications to map burned areas, burn severity and forest patterns in post-fire environments. However, a number of challenges remain, such as how to understand the temporal and spatial dynamics of post-fire environments and ecological responses and to accurately evaluate the characteristics of post-fire boreal forests using a remote sensing approach (Tables 4, 6 and 9, and Figure 3).

Monitoring fire regimes, including the burned area and burn severity, will help to accurately estimate fire emission and carbon sequestration in boreal forests, as well as to understand the short- and long-term ecological effects of fires. However, the availability and accuracy of burned area and burn severity products in boreal regions are often confounded by environmental conditions, limited instrument capabilities (e.g., resolution and cloud cover), the methods of analysis and the presence (or absence) of official data on the burned area and burn severity. As boreal forests are located in high northern latitudes (generally at latitudes from 50° to 70°N), with a very long period of snow and cloud cover annually, direct observation of a clear land surface for mapping the burned area and burn severity is thus limited by using remote sensing, particularly in using optical remote sensing. This problem is particularly challenging for the goal of mapping the burned area and burn severity during early and late-season fires, when the reflectance signatures of burned areas are altered by snow cover and vegetation phenology. Even though a number of mapping algorithms have been developed for boreal regions, ranging from visual interpretation to automatic burned area and burn severity classification algorithms, the accuracy of burned area estimates and burn severity assessments in boreal regions varied significantly among studies. Therefore, the selection of operational data and methods might be challenging within boreal regions, particularly for reconstructing long-time series of burned areas and burn severity. Remote sensing approaches for mapping burned areas and burn severity also require the overcoming of official fire statistics that are incomplete or biased, as well as the assessment of the severity of field-based burn, respectively. These data are urgently needed within some regions, such as boreal forests located in Eurasia.

Mapping and modeling the complexity of post-fire forest patterns and their changes over time is a key issue in spatial forest ecology that is related to fire. Even though remote sensing has been acknowledged as one of the most powerful methods to map components of vegetation and to estimate their changes over time, this technique has sometimes been demonstrated as an unrealistic and biased representation of post-fire forest patterns. For example, optical remote sensing is less than ideal for understory studies, where the overstory canopy blocks the understory signal. Consequently, characterizing the stages of forest succession, including both early and late successional types, might be challenging using optical sensors. This problem, coupled with the saturation issues of vegetation indices, limits the monitoring of post-fire forest patterns that showed, in most reviewed studies, an underestimation of classes of forest succession and an overestimation of the forest recovery rate. Synthetic aperture radar systems and LiDAR systems are well designed to capture forest structure and may address some issues of passive optical systems; however, the application of these data may require higher costs and remain unavailable for mapping post-fire forest patterns at regional-to-continental scales, especially with LiDAR data. Additionally, the limitation of field observation, as well as the variations of environmental conditions (e.g., soil moisture, topography), vegetation characteristics (e.g., pre- and post- fire vegetation, species characteristic) and disturbance regimes (e.g., fire frequency, fire season and severity) also alter the accuracy of modeling the recovery

of post-fire forests, because the recovery process is determined by the complex interaction of those biotic and abiotic factors.

4.2. Possible Solutions and Opportunities for Future Research

Remote sensing offers an enormous amount of data when monitoring and studying forest ecosystems, and the selection of suitable datasets is crucial for maximizing accuracy and efficiency when doing so. Each sensor system has its own shortcomings and advantages in monitoring post-fire effects and patterns of forest recovery, so synergistic use of active and passive sensors provides opportunities to fully characterize post-fire effects and forest patterns that might be impossible with a single dataset. Additionally, many reviewed studies in this paper have emphasized the importance of multi-temporal optical datasets (e.g., Landsat imagery) for post-fire effects and monitoring forest patterns, since these data can be archived historically, corresponding to each stage of forest dynamics and changes. Therefore, the inclusion of time series datasets will account for the nature and level of disturbances that directly influence patterns of forest regrowth. Given that common generation sensors, such as AVHRR, Landsat, MODIS and SPOT, have both advantages and disadvantages in forest monitoring, there is a need for future research and investigation into the application of other sensors with high spatial resolutions (e.g., QuickBird, IKONOS, unmanned aerial vehicle (UAV)), hyperspectral optical sensors, LiDAR/SAR and even future generations of spaceborne LiDAR missions, such as NASA's DESDynI, ICESat-II, and LIST for monitoring post-fire patterns and effects.

Future research should also consider the suggestions in this paper concerning the methods of remote sensing to eliminate the uncertainties of monitoring post-fire patterns and effects. First, as has been stated by many other researchers (e.g., [20,21,56]), studying fire-related forest ecology using remote sensing involves many different disciplines, processes and phenomena. Researchers should properly define all related terminology, use it consistently and clarify the level of presumption in the methods of measuring post-fire effects and forest patterns through the use of remote sensing. Second, analyzing post-fire effects and forest patterns in boreal forests using remote sensing data requires the development of approaches to account for variations in the spatial and spectral resolution of remotely sensed data, environmental conditions, vegetation characteristics and disturbance regimes. Possible approaches might be either the inclusion of all independent variables in modeling post-fire effects and forest patterns (e.g., using non-parametric analysis) or the stratification of these with similar conditions prior to applying the methods of remote sensing for monitoring post-fire effects and forest recovery patterns. With the development of remote sensing capabilities, the extraction and stratification of those independent factors are possible to obtain freely from remote sensing systems, such as the classification of Landsat and MODIS imagery for vegetation classes [93], the ASTER digital elevation model for topography [173] and MODIS fire products for fire regimes [7]. Third, Rocchini *et al.* [194] recently noted that the methods of remote sensing for mapping ecosystems should account for uncertainty in an explicit manner by using uncertainty-related models, such as fuzzy set theory, spectral unmixing, Bayesian theory and bootstrap-based procedures. The uncertainty-related models will represent forest ecosystems as a manner of a continuum, rather than a discrete boundary, which might provide an unrealistic representation. These approaches are very useful, in particular using

remote sensing to monitor burn severity and patterns of forest recovery in which the community of post-fire vegetation is viewed in classes of a continuum, rather than discrete classes [184,197,198]. Finally, it is necessary to conduct more research on the post-fire effects and forest patterns for boreal regions in Eurasia, such as Russia, northeastern China and Mongolia, because of their considerable contribution to the regional and global balance of carbon and climate change, as well as incomplete and biased estimates on the post-fire effects and forest patterns in these regions. All studies on forest fires and forest patterns that are related to remote sensing are also in great need of field campaigns.

Acknowledgements

Conflict of Interest

The authors declare no conflict of interest

References

1. Food and Agriculture Organization (FAO). Global Forest Resources Assessment 2010—Main Report. In *Food and Agriculture Organization of the United Nations (FAO) Forestry Paper*; FAO: Rome, Italia, 2010; Volume 163.
2. European Association of Remote Sensing Laboratories (EARSEL). Disaster Management and Emergency Response in the Mediterranean Region. In Proceedings of the 1st International Conference on Remote Sensing Techniques in Disaster Management and Emergency Response in the Mediterranean Region, Croatia, 22–24 September 2008; Oluic, M., Ed.; EARSEL: Zagreb, Croatia, 2008.
3. Flannigan, M.; Amiro, B.; Logan, K.; Stocks, B.; Wotton, B. Forest fires and climate change in the 21 st century. *Mitig. Adapt. Strateg. Glob. Chang.* **2006**, *11*, 847–859.
4. Carmenta, R.; Parry, L.; Blackburn, A.; Vermeylen, S.; Barlow, J. Understanding human-fire interactions in tropical forest regions: A case for interdisciplinary research across the natural and social sciences. *Ecol. Soc.* **2011**, *16*, 53–75.
5. Babintseva, R.; Titova, Y.V. Effects of Fire on the Regeneration of Larch forests in the Lake Baikal Basin. In *Fire in Ecosystems of Boreal Eurasia*; Springer: Dordrecht, The Netherlands, 1996; Volume 48, pp. 358–365.
6. Goldammer, J.; Furyaev, V. Fire in Ecosystems of Boreal Eurasia. Ecological Impacts and Links to the Global System. In *Fire in Ecosystems of Boreal Eurasia*; Springer: Dordrecht, The Netherlands, 1996; Volume 48, pp. 1–20.
7. de Groot, W.J.; Cantin, A.S.; Flannigan, M.D.; Soja, A.J.; Gowman, L.M.; Newbery, A. A comparison of Canadian and Russian boreal forest fire regimes. *For. Ecol. Manag.* **2012**, *294*, 23–34.

8. Bélisle, A.C.; Gauthier, S.; Cyr, D.; Bergeron, Y.; Morin, H. Fire regime and old-growth boreal forests in central Quebec, Canada: An ecosystem management perspective. *Silva Fenn.* **2011**, *45*, 889–908.

9. Zyryanova, O.; Abaimov, A.; Bugaenko, T.; Bugaenko, N. Recovery of Forest Vegetation after Fire Disturbance. In *Permafrost Ecosystems*; Springer: Dordrecht, The Netherlands, 2010; pp. 83–96.

10. McCullough, D.G.; Werner, R.A.; Neumann, D. Fire and insects in northern and boreal forest ecosystems of North America 1. *Annu. Rev. Entomol.* **1998**, *43*, 107–127.

11. Volney, W.J.A.; Fleming, R.A. Climate change and impacts of boreal forest insects. *Agric. Ecosyst. Environ.* **2000**, *82*, 283–294.

12. Johnstone, J.F.; Hollingsworth, T.N.; Chapin, F.S.; Mack, M.C. Changes in fire regime break the legacy lock on successional trajectories in Alaskan boreal forest. *Glob. Chang. Biol.* **2010**, *16*, 1281–1295.

13. Yoshikawa, K.; Bolton, W.R.; Romanovsky, V.E.; Fukuda, M.; Hinzman, L.D. Impacts of wildfire on the permafrost in the boreal forests of Interior Alaska. *J. Geophys. Res.: Atmos.* **2002**, *107*, FFR 4:1–FFR 4:14.

14. Kasischke, E.S.; Johnstone, J.F. Variation in postfire organic layer thickness in a black spruce forest complex in interior Alaska and its effects on soil temperature and moisture. *Can. J. For. Res.* **2005**, *35*, 2164–2177.

15. Kane, E.; Kasischke, E.; Valentine, D.; Turetsky, M.; McGuire, A. Topographic influences on wildfire consumption of soil organic carbon in interior Alaska: Implications for black carbon accumulation. *J. Geophys. Res.: Biogeosci.* **2007**, doi: 10.1029/2007JG000458.

16. Barrett, K.; McGuire, A.; Hoy, E.; Kasischke, E. Potential shifts in dominant forest cover in interior Alaska driven by variations in fire severity. *Ecol. Appl.* **2011**, *21*, 2380–2396.

17. Johnstone, J.F.; Chapin, F.S.; Hollingsworth, T.N.; Mack, M.C.; Romanovsky, V.; Turetsky, M. Fire, climate change, and forest resilience in interior Alaska *Can. J. For. Res.* **2010**, *40*, 1302–1312.

18. Kasischke, E.S.; Christensen, N.L., Jr.; Stocks, B.J. Fire, global warming, and the carbon balance of boreal forests. *Ecol. Appl.* **1995**, *5*, 437–451.

19. Sofronov, M.; Volokitina, A. Wildfire Ecology in Continuous Permafrost Zone. In *Permafrost Ecosystems*; Springer: Dordrecht, The Netherlands, 2010; pp. 59–82.

20. Lentile, L.B.; Holden, Z.A.; Smith, A.M.S.; Falkowski, M.J.; Hudak, A.T.; Morgan, P.; Lewis, S.A.; Gessler, P.E.; Benson, N.C. Remote sensing techniques to assess active fire characteristics and post-fire effects. *Int. J. Wildland Fire* **2006**, *15*, 319–345.

21. French, N.H.F.; Kasischke, E.S.; Hall, R.J.; Murphy, K.A.; Verbyla, D.L.; Hoy, E.E.; Allen, J.L. Using Landsat data to assess fire and burn severity in the North American boreal forest region: An overview and summary of results. *Int. J. Wildland Fire* **2008**, *17*, 443–462.

22. Veraverbeke, S.; Lhermitte, S.; Verstraeten, W.W.; Goossens, R. The temporal dimension of differenced Normalized Burn Ratio (dNBR) fire/burn severity studies: The case of the large 2007 Peloponnese wildfires in Greece. *Remote Sens. Environ.* **2010**, *114*, 2548–2563.

23. Seidl, R.; Fernandes, P.M.; Fonseca, T.F.; Gillet, F.; Johnsson, A.M.; Merganicova, K.; Netherer, S.; Arpaci, A.; Bontemps, J.-D.; Bugmann, H.; *et al.* Modelling natural disturbances in forest ecosystems: A review. *Ecol. Model.* **2011**, *222*, 903–924.

24. Mulder, V.; de Bruin, S.; Schaepman, M.; Mayr, T. The use of remote sensing in soil and terrain mapping—A review. *Geoderma* **2012**, *122*, 66–74.

25. Hansen, M.C.; Loveland, T.R. A review of large area monitoring of land cover change using Landsat data. *Remote Sens. Environ.* **2012**, *122*, 66–74.

26. Pierce, K.B., Jr.; Ohmann, J.L.; Wimberly, M.C.; Gregory, M.J.; Fried, J.S. Mapping wildland fuels and forest structure for land management: A comparison of nearest neighbor imputation and other methods. *Can. J. For. Res.* **2009**, *39*, 1901–1916.

27. Boyd, D.; Foody, G. An overview of recent remote sensing and GIS based research in ecological informatics. *Ecol. Inf.* **2010**, *6*, 25–36.

28. Powell, S.L.; Cohen, W.B.; Healey, S.P.; Kennedy, R.E.; Moisen, G.G.; Pierce, K.B.; Ohmann, J.L. Quantification of live aboveground forest biomass dynamics with Landsat time-series and field inventory data: A comparison of empirical modeling approaches. *Remote Sens. Environ.* **2010**, *114*, 1053–1068.

29. Wang, S.; Miao, L.; Peng, G. An improved algorithm for forest fire detection using HJ data. *Proced. Environ. Sci.* **2012**, *13*, 140–150.

30. Schroeder, W.; Prins, E.; Giglio, L.; Csiszar, I.; Schmidt, C.; Morisette, J.; Morton, D. Validation of GOES and MODIS active fire detection products using ASTER and ETM+ data. *Remote Sens. Environ.* **2008**, *112*, 2711–2726.

31. Giglio, L.; Csiszar, I.; Restas, A.; Morisette, J.T.; Schroeder, W.; Morton, D.; Justice, C.O. Active fire detection and characterization with the Advanced Spaceborne Thermal Emission and Reflection radiometer (ASTER). *Remote Sens. Environ.* **2008**, *112*, 3055–3063.

32. Wooster, M.; Xu, W.; Nightingale, T. Sentinel-3 SLSTR active fire detection and FRP product: Pre-launch algorithm development and performance evaluation using MODIS and ASTER datasets. *Remote Sens. Environ.* **2012**, *120*, 236–254.

33. Justice, C.O.; Giglio, L.; Roy, D.; Boschetti, L.; Csiszar, I.; Davies, D.; Korontzi, S.; Schroeder, W.; O'Neal, K.; Morisette, J. MODIS-Derived Global Fire Products. In *Land Remote Sensing and Global Environmental Change*; Ramachandran, B., Justice, C.O., Abrams, M.J., Eds.; Springer: New York, NY, USA, 2011; Volume 11, pp. 661–679.

34. Leon, J.R.R.; van Leeuwen, W.J.D.; Casady, G.M. Using MODIS-NDVI for the modeling of post-wildfire vegetation response as a function of environmental conditions and pre-fire restoration treatments. *Remote Sens.* **2012**, *4*, 598–621.

35. Schoennagel, T.; Veblen, T.T.; Romme, W.H. The interaction of fire, fuels, and climate across Rocky Mountain forests. *BioScience* **2004**, *54*, 661–676.

36. Johnson, E.; Miyanishi, K.; Bridge, S. Wildfire regime in the boreal forest and the idea of suppression and fuel buildup. *Conserv. Biol.* **2001**, *15*, 1554–1557.

37. Chuvieco, E.; Congalton, R.G. Application of remote sensing and geographic information systems to forest fire hazard mapping. *Remote Sens. Environ.* **1989**, *29*, 147–159.

38. Liang, J.; Zhou, M.; Verbyla, D.L.; Zhang, L.; Springsteen, A.L.; Malone, T. Mapping forest dynamics under climate change: A matrix model. *For. Ecol. Manag.* **2011**, *262*, 2250–2262.

39. Conard, S.G.; A. Ivanova, G. Wildfire in Russian boreal forests—Potential impacts of fire regime characteristics on emissions and global carbon balance estimates. *Environ. Pollut.* **1997**, *98*, 305–313.

40. Beuning, K.R.M.; Zimmerman, K.A.; Ivory, S.J.; Cohen, A.S. Vegetation response to glacial-interglacial climate variability near Lake Malawi in the southern African tropics. *Palaeogeogr. Palaeoclim. Palaeoecol.* **2011**, *303*, 81–92.

41. Kayes, L.J.; Puettmann, K.J.; Anderson, P.D. Short term bryoid and vascular vegetation response to reforestation alternatives following wildfire in conifer plantations. *Appl. Veg. Sci.* **2011**, *14*, 326–339.

42. Voepel, H.; Ruddell, B.; Schumer, R.; Troch, P.A.; Brooks, P.D.; Neal, A.; Durcik, M.; Sivapalan, M. Quantifying the role of climate and landscape characteristics on hydrologic partitioning and vegetation response. *Water Resour. Res.* **2011**, *47*, W00J09.

43. Russell-Smith, J.; Gardener, M.R.; Brock, C.; Brennan, K.; Yates, C.P.; Grace, B. Fire persistence traits can be used to predict vegetation response to changing fire regimes at expansive landscape scales—An Australian example. *J. Biogeogr.* **2012**, *39*, 1657–1668.

44. Jain, T.B.; Graham, R.T.; Pilliod, D.S. Tongue-tied: Confused meanings for common fire terminology can lead to fuels mismanagement. *Wildfire* **2004**, *6/7*, 22–26.

45. Key, C.H.; Benson, N.C. *Landscape Assessment Sampling and Analysis Methods*; General Technical Report RMRS-GRT-164-CD; USDA Forest Service, Rocky Mountain Research Station: Ogden, UT, USA, 2006.

46. Veraverbeke, S.; Verstraeten, W.W.; Lhermitte, S.; Goossens, R. Evaluating Landsat Thematic Mapper spectral indices for estimating burn severity of the 2007 Peloponnese wildfires in Greece. *Int. J. Wildland Fire* **2010**, *19*, 558–569.

47. Paz, S.; Carmel, Y.; Jahshan, F.; Shoshany, M. Post-fire analysis of pre-fire mapping of fire-risk: A recent case study from Mt. Carmel (Israel). *For. Ecol. Manag.* **2011**, *262*, 1184–1188.

48. Chuvieco, E.; Aguado, I.; Yebra, M.; Nieto, H.; Salas, J.; Martín, M.P.; Vilar, L.; Martínez, J.; Martín, S.; Ibarra, P. Development of a framework for fire risk assessment using remote sensing and geographic information system technologies. *Ecol. Model.* **2010**, *221*, 46–58.

49. Chowdhury, E.H.; Hassan, Q.K. Use of remote sensing-derived variables in developing a forest fire danger forecasting system. *Nat. Hazard.* **2013**, doi: 10.1007/s11069-013-0564-7.

50. Akther, M.; Hassan, Q.K. Remote sensing-based assessment of fire danger conditions over boreal forest. *IEEE J. Sel. Top. Appl. Earth Obs. Remote Sens.* **2011**, *4*, 992–999.

51. Lutz, J.A.; Key, C.; Kolden, C.; Kane, J.; van Wagtendonk, J. Fire frequency, area burned, and severity: A quantitative approach to defining a normal fire year. *Fire Ecol.* **2011**, *7*, 51–65.

52. Roder, A.; Hill, J.; Duguy, B.; Alloza, J.A.; Vallejo, R. Using long time series of Landsat data to monitor fire events and post-fire dynamics and identify driving factors. A case study in the Ayora region (eastern Spain). *Remote Sens. Environ.* **2008**, *112*, 259–273.

53. Senici, D.; Chen, H.Y.; Bergeron, Y.; Cyr, D. Spatiotemporal variations of fire frequency in central boreal forest. *Ecosystems* **2010**, *13*, 1227–1238.

54. Díaz-Delgado, R.; Pons, X. Spatial patterns of forest fires in Catalonia (NE of Spain) along the period 1975–1995: Analysis of vegetation recovery after fire. *For. Ecol. Manag.* **2001**, *147*, 67–74.

55. Brown, C.; Johnstone, J. How does increased fire frequency affect carbon loss from fire? A case study in the northern boreal forest. *Int. J. Wildland Fire* **2011**, *20*, 829–837.

56. Keeley, J.E. Fire intensity, fire severity and burn severity: A brief review and suggested usage. *Int. J. Wildland Fire* **2009**, *18*, 116–126.

57. Heward, H.; Smith, A.M.S.; Roy, D.P.; Tinkham, W.T.; Hoffman, C.M.; Morgan, P.; Lannom, K.O. Is burn severity related to fire intensity? Observations from landscape scale remote sensing. *Int. J. Wildland Fire* **2013**, *22*, 910–918.

58. Barrett, K.; Kasischke, E.S. Controls on variations in MODIS fire radiative power in Alaskan boreal forests: Implications for fire severity conditions. *Remote Sens. Environ.* **2013**, *130*, 171–181.

59. Loboda, T.; French, N.; Hight-Harf, C.; Jenkins, L.; Miller, M. Mapping fire extent and burn severity in Alaskan tussock tundra: An analysis of the spectral response of tundra vegetation to wildland fire. *Remote Sens. Environ.* **2013**, *134*, 194–209.

60. Veraverbeke, S.; Harris, S.; Hook, S. Evaluating spectral indices for burned area discrimination using MODIS/ASTER (MASTER) airborne simulator data. *Remote Sens. Environ.* **2011**, *115*, 2702–2709.

61. Moreno Ruiz, J.A.; Riano, D.; Arbelo, M.; French, N.H.; Ustin, S.L.; Whiting, M.L. Burned area mapping time series in Canada (1984–1999) from NOAA-AVHRR LTDR: A comparison with other remote sensing products and fire perimeters. *Remote Sens. Environ.* **2012**, *117*, 407–414.

62. Kasischke, E.S.; Loboda, T.; Giglio, L.; French, N.H.; Hoy, E.; de Jong, B.; Riano, D. Quantifying burned area for North American forests: Implications for direct reduction of carbon stocks. *J. Geophys. Res.* **2011**, *116*, G04003.

63. George, C.; Rowland, C.; Gerard, F.; Balzter, H. Retrospective mapping of burnt areas in Central Siberia using a modification of the normalised difference water index. *Remote Sens. Environ.* **2006**, *104*, 346–359.

64. Loboda, T.; O'neal, K.; Csiszar, I. Regionally adaptable dNBR-based algorithm for burned area mapping from MODIS data. *Remote Sens. Environ.* **2007**, *109*, 429–442.

65. Kasischke, E.S.; French, N.H. Locating and estimating the areal extent of wildfires in Alaskan boreal forests using multiple-season AVHRR NDVI composite data. *Remote Sens. Environ.* **1995**, *51*, 263–275.

66. Kasischke, E.S.; Turetsky, M.R.; Ottmar, R.D.; French, N.H.; Hoy, E.E.; Kane, E.S. Evaluation of the composite burn index for assessing fire severity in Alaskan black spruce forests. *Int. J. Wildland Fire* **2008**, 17, 515–526.

67. Barrett, K.; Kasischke, E.; McGuire, A.; Turetsky, M.; Kane, E. Modeling fire severity in black spruce stands in the Alaskan boreal forest using spectral and non-spectral geospatial data. *Remote Sens. Environ.* **2010**, *114*, 1494–1503.

68. Boby, L.A.; Schuur, E.A.; Mack, M.C.; Verbyla, D.; Johnstone, J.F. Quantifying fire severity, carbon, and nitrogen emissions in Alaska's boreal forest. *Ecol. Appl.* **2010**, *20*, 1633–1647.

69. Hoy, E.E.; French, N.H.; Turetsky, M.R.; Trigg, S.N.; Kasischke, E.S. Evaluating the potential of Landsat TM/ETM+ imagery for assessing fire severity in Alaskan black spruce forests. *Int. J. Wildland Fire* **2008**, *17*, 500–514.

70. Murphy, K.A.; Reynolds, J.H.; Koltun, J.M. Evaluating the ability of the differenced Normalized Burn Ratio (dNBR) to predict ecologically significant burn severity in Alaskan boreal forests. *Int. J. Wildland Fire* **2008**, *17*, 490–499.

71. Allen, J.L.; Sorbel, B. Assessing the differenced Normalized Burn Ratio's ability to map burn severity in the boreal forest and tundra ecosystems of Alaska's national parks. *Int. J. Wildland Fire* **2008**, *17*, 463–475.

72. Eidenshink, J.; Schwind, B.; Brewer, K.; Zhu, Z.L.; Quayle, B.; Howard, S. A project for monitoring trends in burn severity. *Fire Ecol.* **2007**, *3*, 3–20.

73. Veraverbeke, S.; Lhermitte, S.; Verstraeten, W.W.; Goossens, R. Evaluation of pre/post-fire differenced spectral indices for assessing burn severity in a Mediterranean environment with Landsat Thematic Mapper. *Int. J. Remote Sens.* **2011**, *32*, 3521–3537.

74. Johnstone, J.F.; Kasischke, E.S. Stand-level effects of soil burn severity on postfire regeneration in a recently burned black spruce forest. *Can. J. For. Res.* **2005**, *35*, 2151–2163.

75. Duffy, P.A.; Epting, J.; Graham, J.M.; Rupp, T.S.; McGuire, A.D. Analysis of Alaskan burn severity patterns using remotely sensed data. *Int. J. Wildland Fire* **2007**, *16*, 277–284.

76. Epting, J.; Verbyla, D.; Sorbel, B. Evaluation of remotely sensed indices for assessing burn severity in interior Alaska using Landsat TM and ETM+. *Remote Sens. Environ.* **2005**, *96*, 328–339.

77. Michalek, J.; French, N.; Kasischke, E.; Johnson, R.; Colwell, J. Using Landsat TM data to estimate carbon release from burned biomass in an Alaskan spruce forest complex. *Int. J. Remote Sens.* **2000**, *21*, 323–338.

78. McElhinny, C.; Gibbons, P.; Brack, C.; Bauhus, J. Forest and woodland stand structural complexity: Its definition and measurement. *For. Ecol. Manag.* **2005**, *218*, 1–24.

79. Pommerening, A. Approaches to quantifying forest structures. *Forestry* **2002**, *75*, 305–324.

80. Hollingsworth, T.N.; Johnstone, J.F.; Bernhardt, E.L.; Chapin, F.S., III. Fire severity filters regeneration traits to shape community assembly in Alaska's boreal forest. *PLoS One* **2013**, *8*, e56033.

81. Hicke, J.A.; Asner, G.P.; Kasischke, E.S.; French, N.H.; Randerson, J.T.; James Collatz, G.; Stocks, B.J.; Tucker, C.J.; Los, S.O.; Field, C.B. Postfire response of North American boreal forest net primary productivity analyzed with satellite observations. *Glob. Chang. Biol.* **2003**, *9*, 1145–1157.

82. Furyaev, V.V.V.; Vaganov, E.A.; Tchebakova, N.M.; Valendik, E.N. Effects of fire and climate on successions and structural changes in the Siberian Boreal forest. *Eurasian J. For. Res.* **2001**, *2*, 1–15.

83. Epting, J.; Verbyla, D. Landscape-level interactions of prefire vegetation, burn severity, and postfire vegetation over a 16-year period in interior Alaska. *Can. J. For. Res.* **2005**, *35*, 1367–1377.

84. Schimmel, J.; Granstram, A. Fire severity and vegetation response in the boreal Swedish forest. *Ecology* **1996**, *77*, 1436–1450.

85. Brown, P.M.; Kaufmann, M.R.; Shepperd, W.D. Long-term, landscape patterns of past fire events in a montane ponderosa pine forest of central Colorado. *Landsc. Ecol.* **1999**, *14*, 513–532.

86. Flannigan, M.; Stocks, B.J.; Wotton, B. Climate change and forest fires. *Sci. Total Environ.* **2000**, *262*, 221–229.

87. Huang, F.; Wang, P. Vegetation change of ecotone in west of Northeast China plain using time-series remote sensing data. *Chin. Geogr. Sci.* **2010**, *20*, 167–175.

88. Franklin, J.F.; Spies, T.A.; Pelt, R.V.; Carey, A.B.; Thornburgh, D.A.; Berg, D.R.; Lindenmayer, D.B.; Harmon, M.E.; Keeton, W.S.; Shaw, D.C. Disturbances and structural development of natural forest ecosystems with silvicultural implications, using Douglas-fir forests as an example. *For. Ecol. Manag.* **2002**, *155*, 399–423.

89. Bergeron, Y.; Gauthier, S.; Kafka, V.; Lefort, P.; Lesieur, D. Natural fire frequency for the eastern Canadian boreal forest: Consequences for sustainable forestry. *Can. J. For. Res.* **2001**, *31*, 384–391.

90. Kasischke, E.S.; Bourgeau-Chavez, L.L.; Johnstone, J.F. Assessing spatial and temporal variations in surface soil moisture in fire-disturbed black spruce forests in Interior Alaska using spaceborne synthetic aperture radar imagery—Implications for post-fire tree recruitment. *Remote Sens. Environ.* **2007**, *108*, 42–58.

91. Quintano, C.; Fernandez-Manso, A.; Stein, A.; Bijker, W. Estimation of area burned by forest fires in Mediterranean countries: A remote sensing data mining perspective. *For. Ecol. Manag.* **2011**, *262*, 1597–1607.

92. Loboda, T.V.; Zhang, Z.; O'Neal, K.J.; Sun, G.; Csiszar, I.A.; Shugart, H.H.; Sherman, N.J. Reconstructing disturbance history using satellite-based assessment of the distribution of land cover in the Russian Far East. *Remote Sens. Environ.* **2012**, *118*, 241–248.

93. Potapov, P.; Hansen, M.C.; Stehman, S.V.; Loveland, T.R.; Pittman, K. Combining MODIS and Landsat imagery to estimate and map boreal forest cover loss. *Remote Sens. Environ.* **2008**, *112*, 3708–3719.

94. Earth Explorer. Available online:. Available online: http://earthexplorer.usgs.gov/ (accessed on 15 September 2013).

95. Bourgeau-Chavez, L.; Kasischke, E.; Brunzell, S.; Mudd, J.; Tukman, M. Mapping fire scars in global boreal forests using imaging radar data. *Int. J. Remote Sens.* **2002**, *23*, 4211–4234.

96. Bourgeau-Chavez, L.; Harrell, P.; Kasischke, E.; French, N. The detection and mapping of Alaskan wildfires using a spaceborne imaging radar system. *Int. J. Remote Sens.* **1997**, *18*, 355–373.

97. ASTER: Advanced Spaceborne Thermal Emission and Reflection Radiometer. Available online: http://asterweb.jpl.nasa.gov/ (accessed on 15 September 2013).

98. MODIS. Available online: http://modis.gsfc.nasa.gov (accessed on 15 September 2013).

99. Reverb|ECHO. Available online: http://reverb.echo.nasa.gov (accessed on 15 September 2013).

100. NOAA's Comprehensive Large Array—Data Stewardship System. Available online: http://www.nsof.class.noaa.gov (accessed on 15 September 2013).

101. VEGETATION. Available online: http://www.spot-vegetation.com (accessed on 15 September 2013).

102. Modis Burned area Product Index. Available online: http://modis-fire.umd.edu/Burned_Area_Products.html (accessed on 15 September 2013).

103. Global Fire Emissions Database. Available online: http://www.falw.vu/~gwerf/GFED (accessed on 15 September 2013).

104. GEM—Global Environment Monitoring. Available online: http://bioval.jrc.ec.europa.eu (accessed on 15 September 2013).

105. ESA—Data User Element. Available online: http://dup.esrin.esa.int/prjs/prjs43.php (accessed on 15 September 2013).

106. Geoland2. Available online: http://www.geoland2.eu (accessed on 15 September 2013).

107. Kasischke, E.S.; French, N.H.F.; Harrell, P.; Christensen, N.L., Jr.; Ustin, S.L.; Barry, D. Monitoring of wildfires in boreal forests using large area AVHRR NDVI composite image data. *Remote Sens. Environ.* **1993**, *45*, 61–71.

108. Cahoon, D.R.; Stocks, B.J.; Levine, J.S.; Cofer, W.R.; Pierson, J.M. Satellite analysis of the severe 1987 forest fires in northern China and southeastern Siberia. *J. Geophys. Res.: Atmos.* **1994**, *99*, 18627–18638.

109. French, N.; Kasischke, E.; Bourgeau-Chavez, L.; Berry, D. Mapping the location of wildfires in Alaskan boreal forests using AVHRR imagery. *Int. J. Wildland Fire.* **1995**, *5*, 55–62.

110. Fraser, R.; Li, Z.; Cihlar, J. Hotspot and NDVI differencing synergy (HANDS): A new technique for burned area mapping over boreal forest. *Remote Sens. Environ.* **2000**, *74*, 362–376.

111. Remmel, T.K.; Perera, A.H. Fire mapping in a northern boreal forest: Assessing AVHRR/NDVI methods of change detection. *For. Ecol. Manag.* **2001**, *152*, 119–129.

112. Fraser, R.; Li, Z. Estimating fire-related parameters in boreal forest using SPOT VEGETATION. *Remote Sens. Environ.* **2002**, *82*, 95–110.

113. Li, Z.; Nadon, S.; Cihlar, J. Satellite-based detection of Canadian boreal forest fires: Development and application of the algorithm. *Int. J. Remote Sens.* **2000**, *21*, 3057–3069.

114. Kajii, Y.; Kato, S.; Streets, D.G.; Tsai, N.Y.; Shvidenko, A.; Nilsson, S.; McCallum, I.; Minko, N.P.; Abushenko, N.; Altyntsev, D. Boreal forest fires in Siberia in 1998: Estimation of area burned and emissions of pollutants by advanced very high resolution radiometer satellite data. *J. Geophys. Res.* **2002**, *107*, ACH 4-1–ACH 4-8.

115. Kelhä, V.; Rauste, Y.; Häme, T.; Sephton, T.; Buongiorno, A.; Frauenberger, O.; Soini, K.; Venäläinen, A.; Miguel-Ayanz, J.S.; Vainio, T. Combining AVHRR and ATSR satellite sensor data for operational boreal forest fire detection. *Int. J. Remote Sens.* **2003**, *24*, 1691–1708.

116. Zhang, Y.H.; Wooster, M.J.; Tutubalina, O.; Perry, G.L.W. Monthly burned area and forest fire carbon emission estimates for the Russian Federation from SPOT VGT. *Remote Sens. Environ.* **2003**, *87*, 1–15.

117. Soja, A.; Sukhinin, A.; Cahoon, D., Jr.; Shugart, H.; Stackhouse, P., Jr. AVHRR-derived fire frequency, distribution and area burned in Siberia. *Int. J. Remote Sens.* **2004**, *25*, 1939–1960.

118. Sukhinin, A.I.; French, N.H.; Kasischke, E.S.; Hewson, J.H.; Soja, A.J.; Csiszar, I.A.; Hyer, E.J.; Loboda, T.; Conrad, S.G.; Romasko, V.I. AVHRR-based mapping of fires in Russia: New products for fire management and carbon cycle studies. *Remote Sens. Environ.* **2004**, *93*, 546–564.

119. Loboda, T.; Csiszar, I. Reconstruction of fire spread within wildland fire events in Northern Eurasia from the MODIS active fire product. *Glob. Planet. Chang.* **2007**, *56*, 258–273.

120. Pu, R.; Li, Z.; Gong, P.; Csiszar, I.; Fraser, R.; Hao, W.-M.; Kondragunta, S.; Weng, F. Development and analysis of a 12-year daily 1-km forest fire dataset across North America from NOAA/AVHRR data. *Remote Sens. Environ.* **2007**, *108*, 198–208.

121. Chuvieco, E.; Englefield, P.; Trishchenko, A.P.; Luo, Y. Generation of long time series of burn area maps of the boreal forest from NOAA—AVHRR composite data. *Remote Sens. Environ.* **2008**, *112*, 2381–2396.

122. Loboda, T.V.; Hoy, E.E.; Giglio, L.; Kasischke, E.S. Mapping burned area in Alaska using MODIS data: A data limitations-driven modification to the regional burned area algorithm. *Int. J. Wildland Fire.* **2011**, *20*, 487–496.

123. Vivchar, A. Wildfires in Russia in 2000–2008: Estimates of burnt areas using the satellite MODIS MCD45 data. *Remote Sens. Lett.* **2011**, *2*, 81–90.

124. Erdenesaikhan, N.; Erdenetuya, M. Forest and steppe fire monitoring in Mongolia using satellite remote sensing. *Int. Forest Fire News* **1999**, *21*, 71–74.

125. Chuvieco, E.; Opazo, S.; Sione, W.; Valle, H.D.; Anaya, J.; Bella, C.D.; Cruz, I.; Manzo, L.; Lopez, G.; Mari, N. Global burned-land estimation in Latin America using MODIS composite data. *Ecol. Appl.* **2008**, *18*, 64–79.

126. Roy, D.; Boschetti, L.; Justice, C.; Ju, J. The collection 5 MODIS burned area product—Global evaluation by comparison with the MODIS active fire product. *Remote Sens. Environ.* **2008**, *112*, 3690–3707.

127. Giglio, L.; Loboda, T.; Roy, D.P.; Quayle, B.; Justice, C.O. An active-fire based burned area mapping algorithm for the MODIS sensor. *Remote Sens. Environ.* **2009**, *113*, 408–420.

128. Loepfe, L.; Lloret, F.; Roman-Cuesta, R.M. Comparison of burnt area estimates derived from satellite products and national statistics in Europe. *Int. J. Remote Sens.* **2012**, *33*, 3653–3671.

129. Giglio, L.; Randerson, J.; Werf, G.; Kasibhatla, P.; Collatz, G.; Morton, D.; DeFries, R. Assessing variability and long-term trends in burned area by merging multiple satellite fire products. *Biogeosciences* **2010**, *7*, 1171–1186.

130. Chuvieco, E.; Giglio, L.; Justice, C. Global characterization of fire activity: Toward defining fire regimes from Earth observation data. *Glob. Chang. Biol.* **2008**, *14*, 1488–1502.

131. Tansey, K.; Grégoire, J.M.; Defourny, P.; Leigh, R.; Pekel, J.F.; van Bogaert, E.; Bartholomé, E. A new, global, multi-annual (2000–2007) burnt area product at 1 km resolution. *Geophys. Res. Lett.* **2008**, *35*, L01401.

132. Grégoire, J.-M.; Tansey, K.; Silva, J. The GBA2000 initiative: Developing a global burnt area database from SPOT-VEGETATION imagery. *Int. J. Remote Sens.* **2003**, *24*, 1369–1376.

133. Tansey, K.; Grégoire, J.M.; Stroppiana, D.; Sousa, A.; Silva, J.; Pereira, J.; Boschetti, L.; Maggi, M.; Brivio, P.A.; Fraser, R. Vegetation burning in the year 2000: Global burned area estimates from SPOT VEGETATION data. *J. Geophys. Res.: Atmos.* **2004**, *109*, D14S03.

134. Giglio, L.; Randerson, J.T.; van der Werf, G.R. Analysis of daily, monthly, and annual burned area using the fourth-generation global fire emissions database (GFED4). *J. Geophys. Res.: Biogeosci.* **2013**, *118*, 317–328.

135. Plummer, S.; Arino, O.; Simon, M.; Steffen, W. Establishing a earth observation product service for the terrestrial carbon community: The GLOBCARBON initiative. *Mitig. Adapt. Strateg. Glob. Chang.* **2006**, *11*, 97–111.

136. Lacaze, R.; Balsamo, G.; Baret, F.; Bradley, A.; Calvet, J.; Camacho, F.; D'Andrimont, R.; Freitas, S.; Makhmara, H.; Naeimi, V. Geoland2-Towards an Operational GMES Land Monitoring Core Service; First Results of the Biogeophysical Parameter Core Mapping Service.

In Proceedings of the ISPRS TC VII Symposium—100 Years ISPRS, Vienna, Austria, 5–7 July 2010; pp. 354–359.

137. Carmona-Moreno, C.; Belward, A.; Malingreau, J.P.; Hartley, A.; Garcia-Alegre, M.; Antonovskiy, M.; Buchshtaber, V.; Pivovarov, V. Characterizing interannual variations in global fire calendar using data from Earth observing satellites. *Glob. Chang. Biol.* **2005**, *11*, 1537–1555.

138. Soverel, N.O.; Perrakis, D.D.B.; Coops, N.C. Estimating burn severity from Landsat dNBR and RdNBR indices across western Canada. *Remote Sens. Environ.* **2010**, *114*, 1896–1909.

139. Kukavskaya, E.A.; Soja, A.J.; Petkov, A.P.; Ponomarev, E.I.; Ivanova, G.A.; Conard, S.G. Fire emissions estimates in Siberia: Evaluation of uncertainties in area burned, land cover, and fuel consumption. *Can. J. For. Res.* **2012**, *43*, 493–506.

140. Mouillot, F.; Schultz, M.G.; Yue, C.; Cadule, P.; Tansey, K.; Ciais, P.; Chuvieco, E. Ten years of global burned area products from spaceborne remote sensing—A review: Analysis of user needs and recommendations for future developments. *Int. J. Appl. Earth Obs. Geoinf.* **2014**, *26*, 64–79.

141. Miller, J.D.; Thode, A.E. Quantifying burn severity in a heterogeneous landscape with a relative version of the delta Normalized Burn Ratio (dNBR). *Remote Sens. Environ.* **2007**, *109*, 66–80.

142. Bastarrika, A.; Chuvieco, E.; Martan, M.P. Mapping burned areas from Landsat TM/ETM+ data with a two-phase algorithm: Balancing omission and commission errors. *Remote Sens. Environ.* **2011**, *115*, 1003–1012.

143. Pereira, J.M.C. A comparative evaluation of NOAA/AVHRR vegetation indexes for burned surface detection and mapping. *IEEE Trans. Geosci. Remote Sens.* **1999**, *37*, 217–226.

144. Riaño, D.; Moreno Ruiz, J.; Isidoro, D.; Ustin, S. Global spatial patterns and temporal trends of burned area between 1981 and 2000 using NOAA-NASA Pathfinder. *Glob. Chang. Biol.* **2007**, *13*, 40–50.

145. Liew, S.C.; Lim, O.K.; Kwoh, L.K.; Lim, H. A Study of the 1997 Forest Fires in South East Asia using SPOT Quicklook Mosaics. In Proceedings of 1998 IEEE International Geoscience and Remote Sensing Symposium (IGARSS'98), Seattle, WA, USA, 6–10 Jul 1998; Volume 872, pp. 879–881.

146. Lozano, F.J.; Suarez-Seoane, S.; de Luis, E. Assessment of several spectral indices derived from multi-temporal Landsat data for fire occurrence probability modelling. *Remote Sens. Environ.* **2007**, *107*, 533–544.

147. Morton, D.C.; DeFries, R.S.; Nagol, J.; Souza, C.M., Jr.; Kasischke, E.S.; Hurtt, G.C.; Dubayah, R. Mapping canopy damage from understory fires in Amazon forests using annual time series of Landsat and MODIS data. *Remote Sens. Environ.* **2011**, *115*, 1706–1720.

148. Stroppiana, D.; Bordogna, G.; Carrara, P.; Boschetti, M.; Boschetti, L.; Brivio, P. A method for extracting burned areas from Landsat TM/ETM+ images by soft aggregation of multiple spectral indices and a region growing algorithm. *ISPRS J. Photogramm. Remote Sens.* **2012**, *69*, 88–102.

149. Kasischke, E.S.; Verbyla, D.L.; Rupp, T.S.; McGuire, A.D.; Murphy, K.A.; Jandt, R.; Barnes, J.L.; Hoy, E.E.; Duffy, P.A.; Calef, M. Alaskas changing fire regime implications for the vulnerability of its boreal forests. *Can. J. For.Res.* **2010**, *40*, 1313–1324.

150. Delbart, N.; Le Toan, T.; Kergoat, L.; Fedotova, V. Remote sensing of spring phenology in boreal regions: A free of snow-effect method using NOAA-AVHRR and SPOT-VGT data (1982–2004). *Remote Sens. Environ.* **2006**, *101*, 52–62.

151. Cocke, A.E.; Fule, P.Z.; Crouse, J.E. Comparison of burn severity assessments using differenced normalized burn ratio and ground data. *Int. J. Wildland Fire* **2005**, *14*, 189–198.

152. Rodriguez-Alleres, M.; Varela, M.; Benito, E. Natural severity of water repellency in pine forest soils from NW Spain and influence of wildfire severity on its persistence. *Geoderma* **2012**, *191*, 125–131.

153. Veraverbeke, S.; Verstraeten, W.W.; Lhermitte, S.; van de Kerchove, R.; Goossens, R. Assessment of post-fire changes in land surface temperature and surface albedo, and their relation with fire/burn severity using multitemporal MODIS imagery. *Int. J. Wildland Fire* **2012**, *21*, 243–256.

154. Brewer, C.K.; Winne, J.C.; Redmond, R.L.; Opitz, D.W.; Mangrich, M.V. Classifying and mapping wildfire severity: A comparison of methods. *Photogramm. Eng. Remote Sens.* **2005**, *71*, 1311–1320.

155. Cansler, C.A.; McKenzie, D. How robust are burn severity indices when applied in a new region? Evaluation of alternate field-based and remote-sensing methods. *Remote Sens.* **2012**, *4*, 456–483.

156. Chen, X.; Vogelmann, J.E.; Rollins, M.; Ohlen, D.; Key, C.H.; Yang, L.; Huang, C.; Shi, H. Detecting post-fire burn severity and vegetation recovery using multitemporal remote sensing spectral indices and field-collected composite burn index data in a ponderosa pine forest. *Int. J. Remote Sens.* **2011**, *32*, 7905–7927.

157. Harris, S.; Veraverbeke, S.; Hook, S. Evaluating spectral indices for assessing fire severity in chaparral ecosystems (Southern California) using MODIS/ASTER (MASTER) airborne simulator data. *Remote Sens.* **2011**, *3*, 2403–2419.

158. de Santis, A.; Chuvieco, E. GeoCBI: A modified version of the composite burn index for the initial assessment of the short-term burn severity from remotely sensed data. *Remote Sens. Environ.* **2009**, *113*, 554–562.

159. Verbyla, D.L.; Kasischke, E.S.; Hoy, E.E. Seasonal and topographic effects on estimating fire severity from Landsat TM/ETM+ data. *Int. J. Wildland Fire* **2008**, *17*, 527–534.

160. Jain, T.B.; Pilliod, D.S.; Graham, R.T.; Lentile, L.B.; Sandquist, J.E. Index for characterizing post-fire soil environments in temperate coniferous forests. *Forests* **2012**, *3*, 445–466.

161. Alleaume, S.; Hely, C.; Le Roux, J.; Korontzi, S.; Swap, R.; Shugart, H.; Justice, C. Using MODIS to evaluate heterogeneity of biomass burning in southern African savannahs: A case study in Etosha. *Int. J. Remote Sens.* **2005**, *26*, 4219–4237.

162. Bourgeau-Chavez, L.; Kasischke, E.; French, N.; Szeto, L.; Kherkher, C. Using ERS-1 SAR Imagery to Monitor Variations in Burn Severity in an Alaskan Fire-disturbed Boreal Forest Ecosystem. In Proceedings of the IEEE Geoscience and Remote Sensing Symposium (IGARSS'94)—Surface and Atmospheric Remote Sensing: Technologies, Data Analysis and Interpretation, Pasadena, CA, USA, 8–12 August 1994; Volume 1, pp. 243–245.

163. Walz, Y.; Maier, S.W.; Dech, S.W.; Conrad, C.; Colditz, R.R. Classification of burn severity using Moderate Resolution Imaging Spectroradiometer (MODIS): A case study in the Jarrah-Marri forest of southwest Western Australia. *J. Geophys. Res.* **2007**, *112*, G02002.

164. Boer, M.M.; Macfarlane, C.; Norris, J.; Sadler, R.J.; Wallace, J.; Grierson, P.F. Mapping burned areas and burn severity patterns in SW Australian eucalypt forest using remotely sensed changes in leaf area index. *Remote Sens. Environ.* **2008**, *112*, 4358–4369.

165. Hall, R.J.; Freeburn, J.T.; De Groot, W.J.; Pritchard, J.M.; Lynham, T.J.; Landry, R. Remote sensing of burn severity: Experience from western Canada boreal fires. *Int. J. Wildland Fire* **2008**, *17*, 476–489.

166. Verbyla, D.; Lord, R. Estimating post-fire organic soil depth in the Alaskan boreal forest using the normalized burn ratio. *Int. J. Remote Sens.* **2008**, *29*, 3845–3853.

167. Jin, Y.; Randerson, J.T.; Goetz, S.J.; Beck, P.S.A.; Loranty, M.M.; Goulden, M.L. The influence of burn severity on postfire vegetation recovery and albedo change during early succession in North American boreal forests. *J. Geophys. Res.* **2012**, *117*, G01036.

168. Soverel, N.O.; Coops, N.C.; Perrakis, D.D.B.; Daniels, L.D.; Gergel, S.E. The transferability of a dNBR-derived model to predict burn severity across 10 wildland fires in western Canada. *Int. J. Wildland Fire* **2011**, *20*, 518–531.

169. Cai, W.; Yang, J.; Liu, Z.; Hu, Y.; Weisberg, P.J. Post-fire tree recruitment of a boreal larch forest in Northeast China. *For. Ecol. Manag.* **2013**, *307*, 20–29.

170. Wu, Z.; He, H.; Liang, Y.; Cai, L.; Lewis, B. Determining relative contributions of vegetation and topography to burn severity from LANDSAT imagery. *Environ. Manag.* **2013**, *52*, 821–836.

171. Sorbel, B.; Allen, J. Space-based burn severity mapping in Alaska's national parks. *Alaska Park Sci.* **2005**, *4*, 5–11.

172. de Santis, A.; Chuvieco, E. Burn severity estimation from remotely sensed data: Performance of simulation versus empirical models. *Remote Sens. Environ.* **2007**, *108*, 422–435.

173. Hirano, A.; Welch, R.; Lang, H. Mapping from ASTER stereo image data: DEM validation and accuracy assessment. *ISPRS J. Photogramm. Remote Sens.* **2003**, *57*, 356–370.

174. Sunderman, S.O.; Weisberg, P.J. Remote sensing approaches for reconstructing fire perimeters and burn severity mosaics in desert spring ecosystems. *Remote Sens. Environ.* **2011**, *115*, 2384–2389.

175. Gitas, I.; Mitri, G.; Veraverbeke, S.; Polychronaki, A. Advances in Remote Sensing of Post-Fire Vegetation Recovery Monitoring—A Review. In *Remote Sensing of Biomass—Principles and Applications*; Fatoyinbo, L., Ed.; InTech: Rijeka, Croatia, 2012; Chapter 7; pp. 143–176.

176. Lutz, D.A.; Washington-Allen, R.A.; Shugart, H.H. Remote sensing of boreal forest biophysical and inventory parameters: A review. *Can. J. Remote Sens.* **2008**, *34*, 286–313.

177. Liu, W.; Song, C.; Schroeder, T.A.; Cohen, W.B. Predicting forest successional stages using multitemporal Landsat imagery with forest inventory and analysis data. *Int. J. Remote Sens.* **2008**, *29*, 3855–3872.

178. Zhao, F.J.; Shu, L.F.; Wang, M.Y.; Liu, B.; Yang, L.J. Influencing factors on early vegetation restoration in burned area of *Pinus pumila–Larch* forest. *Acta Ecol. Sinica* **2012**, *32*, 57–61.

179. Dorisuren, C. Post-Fire Successions of the Larch Forests in Mongolia. In Proceedings of the First International Central Asian Wildland Fire Joint Conference and Consultation, Ulaanbaatar, Mongolia, 2–6 June 2008; pp. 24–31.

180. Johnstone, J.F.; Chapin, F., III; Foote, J.; Kemmett, S.; Price, K.; Viereck, L. Decadal observations of tree regeneration following fire in boreal forests. *Can. J. For. Res.* **2004**, *34*, 267–273.

181. Song, C.; Schroeder, T.A.; Cohen, W.B. Predicting temperate conifer forest successional stage distributions with multitemporal Landsat Thematic Mapper imagery. *Remote Sens. Environ.* **2007**, *106*, 228–237.

182. Bergen, K.M.; Dronova, I. Observing succession on aspen-dominated landscapes using a remote sensing-ecosystem approach. *Landsc. Ecol.* **2007**, *22*, 1395–1410.

183. Tanase, M.; de la Riva, J.; Santoro, M.; Pérez-Cabello, F.; Kasischke, E. Sensitivity of SAR data to post-fire forest regrowth in Mediterranean and boreal forests. *Remote Sens. Environ.* **2011**, *115*, 2075–2085.

184. Vehmas, M.; Eerikäinen, K.; Peuhkurinen, J.; Packalén, P.; Maltamo, M. Airborne laser scanning for the site type identification of mature boreal forest stands. *Remote Sens.* **2011**, *3*, 100–116.

185. Vehmas, M.; Eerikäinen, K.; Peuhkurinen, J.; Packalén, P.; Maltamo, M. Identification of boreal forest stands with high herbaceous plant diversity using airborne laser scanning. *For. Ecol. Manag.* **2009**, *257*, 46–53.

186. Falkowski, M.J.; Evans, J.S.; Martinuzzi, S.; Gessler, P.E.; Hudak, A.T. Characterizing forest succession with lidar data: An evaluation for the Inland Northwest, USA. *Remote Sens. Environ.* **2009**, *113*, 946–956.

187. Zhang, Q.; Pavlic, G.; Chen, W.; Latifovic, R.; Fraser, R.; Cihlar, J. Deriving stand age distribution in boreal forests using SPOT VEGETATION and NOAA AVHRR imagery. *Remote Sens. Environ.* **2004**, *91*, 405–418.

188. Hall, F.G.; Botkin, D.B.; Strebel, D.E.; Woods, K.D.; Goetz, S.J. Large-scale patterns of forest succession as determined by remote sensing. *Ecology* **1991**, *72*, 628–640.

189. Steyaert, L.; Hall, F.; Loveland, T. Land cover mapping, fire regeneration, and scaling studies in the Canadian boreal forest with 1 km AVHRR and Landsat TM data. *J. Geophys. Res.* **1997**, *102*, 29581–29529.

190. Fiorella, M.; Ripple, W.J. Determining successional stage of temperate coniferous forests with Landsat satellite data. *Photogramm. Eng. Remote Sens.* **1993**, *59*, 239–246.

191. Foody, G.M.; Palubinskas, G.; Lucas, R.M.; Curran, P.J.; Honzak, M. Identifying terrestrial carbon sinks: Classification of successional stages in regenerating tropical forest from Landsat TM data. *Remote Sens. Environ.* **1996**, *55*, 205–216.

192. Jakubauskas, M.E. Thematic Mapper characterization of lodgepole pine seral stages in Yellowstone National Park, USA. *Remote Sens. Environ.* **1996**, *56*, 118–132.

193. Vicente-Serrano, S.M.; Perez-Cabello, F.; Lasanta, T. *Pinus halepensis* regeneration after a wildfire in a semiarid environment: Assessment using multitemporal Landsat images. *Int. J. Wildland Fire* **2010**, *20*, 195–208.

194. Rocchini, D.; Foody, G.M.; Nagendra, H.; Ricotta, C.; Anand, M.; He, K.S.; Amici, V.; Kleinschmit, B.; Förster, M.; Schmidtlein, S. Uncertainty in ecosystem mapping by remote sensing. *Comput. Geosci.* **2013**, *50*, 128–135.

195. Lucas, R.; Clewley, D.; Rosenqvist, A.; Kellndorfer, J.; Walker, W.; Hoekman, D.; Shimada, M.; de Mesquita, H.N., Jr. Global Forest Monitoring with Synthetic Aperture Radar (SAR) Data. In *Global Forest Monitoring from Earth Observation*; Achard, F., Hansen, M.C., Eds.; CRC Press: Boca Raton, FL, USA, 2012; pp. 287–312.

196. Kasischke, E.S.; Tanase, M.A.; Bourgeau-Chavez, L.L.; Borr, M. Soil moisture limitations on monitoring boreal forest regrowth using spaceborne L-band SAR data. *Remote Sens. Environ.* **2011**, *115*, 227–232.

197. Franklin, S.E. Using Forest Successional Classes. In *Remote Sensing for Sustainable Forest Management*; CRC Press: Boca Raton, FL, USA, 2001; pp. 232–233.

198. Ustin, S.L.; Gamon, J.A. Remote sensing of plant functional types. *New Phytol.* **2010**, *186*, 795–816.

199. Li, H.; Gartner, D.I.; Mou, P.; Trettin, C.C. A landscape model (LEEMATH) to evaluate effects of management impacts on timber and wildlife habitat. *Comput. Electron. Agric.* **2000**,*27*, 263–292.

200. O'Hara, K.L.L., Penelope A.; Hessburg, P.; Smith, B.G. A structural classification for inland northwest forest vegetation. *Western J. Appl. For.* **1996**, *11*, 97–102.

201. Wunderle, A.; Franklin, S.; Guo, X. Age class estimation of western red cedar using SPOT-5 pan-sharpened imagery in British Columbia, Canada. *Geocarto Int.* **2009**, *24*, 47–63.

202. Chen, X.; Vierling, L.; Deering, D.; Conley, A. Monitoring boreal forest leaf area index across a Siberian burn chronosequence: A MODIS validation study. *Int. J. Remote Sens.* **2005**, *26*, 5433–5451.

203. Veraverbeke, S.; Gitas, I.; Katagis, T.; Polychronaki, A.; Somers, B.; Goossens, R. Assessing post-fire vegetation recovery using red-near infrared vegetation indices: Accounting for background and vegetation variability. *ISPRS J. Photogramm. Remote Sens.* **2011**, *68*, 28–39.

204. Berner, L.T.; Beck, P.S.A.; Bunn, A.G.; Lloyd, A.H.; Goetz, S.J. High-latitude tree growth and satellite vegetation indices: Correlations and trends in Russia and Canada (1982–2008). *J. Geophys. Res.* **2010**, *116*, G01015.

205. Kobayashi, H.; Delbart, N.; Suzuki, R.; Kushida, K. A satellite-based method for monitoring seasonality in the overstory leaf area index of Siberian larch forest. *J. Geophys. Res.* **2010**, *115*, G01002.

206. Pflugmacher, D.; Cohen, W.B.; E. Kennedy, R. Using Landsat-derived disturbance history (1972–2010) to predict current forest structure. *Remote Sens. Environ.* **2012**, *122*, 146–165.

207. Selkowitz, D.J.; Green, G.; Peterson, B.; Wylie, B. A multi-sensor lidar, multi-spectral and multi-angular approach for mapping canopy height in boreal forest regions. *Remote Sens. Environ.* **2012**, *121*, 458–471.

208. Magnussen, S.; Wulder, M.A. Post-fire canopy height recovery in Canada's boreal forests using Airborne Laser Scanner (ALS). *Remote Sens.* **2012**, *4*, 1600–1616.

209. Andersen, H.E.; Strunk, J.; Temesgen, H.; Atwood, D.; Winterberger, K. Using multilevel remote sensing and ground data to estimate forest biomass resources in remote regions: A case study in the boreal forests of interior Alaska. *Can. J. Remote Sens.* **2011**, *37*, 596–611.

210. Wulder, M.A.; Han, T.; White, J.C.; Sweda, T.; Tsuzuki, H. Integrating profiling LIDAR with Landsat data for regional boreal forest canopy attribute estimation and change characterization. *Remote Sens. Environ.* **2007**, *110*, 123–137.

211. Wulder, M.; White, J.; Alvarez, F.; Han, T.; Rogan, J.; Hawkes, B. Characterizing boreal forest wildfire with multi-temporal Landsat and LIDAR data. *Remote Sens. Environ.* **2009**, *113*, 1540–1555.

212. Goetz, S.; Sun, M.; Baccini, A.; Beck, P. Synergistic use of spaceborne lidar and optical imagery for assessing forest disturbance: An Alaska case study. *J. Geophys. Res.: Biogeosci.* **2010**, *115*, G00E07.

213. Bourgeau-Chavez, L.; Kasischke, E.; Riordan, K.; Brunzell, S.; Nolan, M.; Hyer, E.; Slawski, J.; Medvecz, M.; Walters, T.; Ames, S. Remote monitoring of spatial and temporal surface soil moisture in fire disturbed boreal forest ecosystems with ERS SAR imagery. *Int. J. Remote Sens.* **2007**, *28*, 2133–2162.

214. Heiskanen, J. Estimating aboveground tree biomass and leaf area index in a mountain birch forest using ASTER satellite data. *Int. J. Remote Sens.* **2006**, *27*, 1135–1158.

215. Heiskanen, J.; Kivinen, S. Assessment of multispectral, -temporal and -angular MODIS data for tree cover mapping in the tundra–taiga transition zone. *Remote Sens. Environ.* **2008**, *112*, 2367–2380.

216. Wolter, P.T.; Townsend, P.A.; Sturtevant, B.R. Estimation of forest structural parameters using 5 and 10 meter SPOT-5 satellite data. *Remote Sens. Environ.* **2009**, *113*, 2019–2036.

217. Li, A.; Huang, C.; Sun, G.; Shi, H.; Toney, C.; Zhu, Z.; Rollins, M.G.; Goward, S.N.; Masek, J.G. Modeling the height of young forests regenerating from recent disturbances in Mississippi using Landsat and ICESat data. *Remote Sens. Environ.* **2011**, *115*, 1837–1849.

218. Young, B.; Liang, J.; Stuart Chapin Iii, F. Effects of species and tree size diversity on recruitment in the Alaskan boreal forest: A geospatial approach. *For. Ecol. Manag.* **2011**, *262*, 1608–1617.

219. Cuevas-González, M.; Gerard, F.; Balzter, H.; Riaño, D. Studying the change in fAPAR after forest fires in Siberia using MODIS. *Int. J. Remote Sens.* **2008**, *29*, 6873–6892.

220. Benson, M.; Pierce, L.; Bergen, K.; Sarabandi, K.; Zhang, K.; Ryan, C. Forest Structure Estimation using SAR, Lidar, and Optical Data in the Canadian Boreal Forest. In Proceedings of IEEE 2011 International Geoscience and Remote Sensing Symposium (IGARSS'01), Vancouver, BC, USA, 24–29 July 2011; pp. 2609–2612.

221. Cuevas Gonzalez, M.; Gerard, F.; Balzter, H.; Riaño, D. Analysing forest recovery after wildfire disturbance in boreal Siberia using remotely sensed vegetation indices. *Glob. Chang. Biol.* **2009**, *15*, 561–577.

222. Kasischke, E.; French, N. Constraints on using AVHRR composite index imagery to study patterns of vegetation cover in boreal forests. *Int. J. Remote Sens.* **1997**, *18*, 2403–2426.

223. Beck, P.S.; Goetz, S.J.; Mack, M.C.; Alexander, H.D.; Jin, Y.; Randerson, J.T.; Loranty, M. The impacts and implications of an intensifying fire regime on Alaskan boreal forest composition and albedo. *Glob. Chang. Biol.* **2011**, *17*, 2853–2866.

224. Lyons, E.A.; Jin, Y.; Randerson, J.T. Changes in surface albedo after fire in boreal forest ecosystems of interior Alaska assessed using MODIS satellite observations. *J. Geophys. Res.* **2008**, *113*, G02012.

225. Goetz, S.J.; Fiske, G.J.; Bunn, A.G. Using satellite time-series data sets to analyze fire disturbance and forest recovery across Canada. *Remote Sens. Environ.* **2006**, *101*, 352–365.

226. Jones, M.O.; Kimball, J.S.; Jones, L.A. Satellite microwave detection of boreal forest recovery from the extreme 2004 wildfires in Alaska and Canada. *Glob. Chang. Biol.* **2013**, *19*, 3111–3122.

227. Alcaraz-Segura, D.; Chuvieco, E.; Epstein, H.E.; Kasischke, E.S.; Trishchenko, A. Debating the greening *vs*. browning of the North American boreal forest: Differences between satellite datasets. *Glob. Chang. Biol.* **2010**, *16*, 760–770.

228. Idris, M.H.; Kuraji, K.; Suzuki, M. Evaluating vegetation recovery following large-scale forest fires in Borneo and northeastern China using multi-temporal NOAA/AVHRR images. *J. For. Res.* **2005**, *10*, 101–111.

229. Frolking, S.; Palace, M.; Clark, D.; Chambers, J.; Shugart, H.; Hurtt, G. Forest disturbance and recovery: A general review in the context of spaceborne remote sensing of impacts on aboveground biomass and canopy structure. *J. Geophys. Res.* **2009**, *114*, G00E02.

230. Buma, B. Evaluating the utility and seasonality of NDVI values for assessing post-disturbance recovery in a subalpine forest. *Environ. Monit. Assess.* **2012**, *184*, 3849–3860.